

Properties of cryogenic insulants

J. Gerhold

Technische Universität Graz, Institut für Elektrische Maschinen und Antriebstechnik,
Kopernikusgasse 24, A-8010 Graz, Austria

Received 27 April 1998; revised 18 June 1998

High vacuum, cold gases and liquids, and solids are the principal insulating materials for superconducting apparatus. All these insulants have been claimed to show fairly good intrinsic dielectric performance under laboratory conditions where small scale experiments in the short term range are typical. However, the insulants must be integrated into large scaled insulating systems which must withstand any particular stressing voltage seen by the actual apparatus over the full life period. Estimation of the amount of degradation needs a reliable extrapolation from small scale experimental data. The latter are reviewed in the light of new experimental data, and guidelines for extrapolation are discussed. No degradation may be seen in resistivity and permittivity. Dielectric losses in liquids, however, show some degradation, and breakdown as a statistical event must be scrutinized very critically. Although information for breakdown strength degradation in large systems is still fragmentary, some thumb rules can be recommended for design. © 1998 Elsevier Science Ltd. All rights reserved

Keywords: dielectric properties; vacuum; fluids; solids; power applications; superconductors

The dielectric insulation design of any superconducting power apparatus must be based on the available insulators. It is mandatory to have a deep knowledge of the properties of insulants in order to meet the required withstand voltage of a system. Standardized voltages and field configurations are common practice in laboratory experiments where the stressed size and stressing time must be limited due to cost reasons. A kind of intrinsic performance can eventually be extrapolated from these experiments.

However, all insulants show degradation in the laboratory performance, where well controlled conditions can be maintained, when used in a practical application. The degradation amount in a system depends on various factors such as stressed size, stressing time, voltage shape, contaminants, voids. System performance can only be estimated from the ideal performance when the particular degradation characteristics are known. Unfortunately, information about multiple stress degradation is incomplete in the low temperature domain; only tendencies for some distinct degradation effects may be defined. The present paper gives a survey of the cryogenic insulator performances which have been measured under laboratory conditions around the world; degradation characteristics are discussed whenever information is available.

There are three pillars for cryogenic insulants:

1. high vacuum;
2. gases and liquids;
3. solids.

Of special interest for normal operation are the resistivity, the permittivity, and the dielectric losses. No breakdown can be allowed at all in order to prevent system damage. Breakdown is a statistical event, and the particular withstand voltage has to be evaluated in accordance with an extremely low breakdown probability, in order to meet the needs for the definite design method¹. *Figure 1* gives a survey of the breakdown strength of various insulants being relevant in applications^{2,3}. There are a sufficient number of cryogenic insulators which match thermal and mechanical performance, and which may support high voltage stress⁴. A list of papers dealing with cryogenic insulation materials and techniques can be found in a review of CIGRE WG-TF 15.06.01⁵.

High vacuum insulation

Vacuum technology is very common in cryogenic systems for thermal insulation. It may be near at hand to utilize vacuum as a dielectric insulation medium, and great efforts have been made in the past to establish practical vacuum-based insulation systems. No problems with thermomechanical mismatch are involved. Application success in the field of cryogenics is limited to the medium voltage range hitherto.

Current flow and breakdown in vacuum at room temperature is reproduced at cryogenic temperatures at somewhat higher voltage in general⁶. An ideal vacuum gap may be assumed at first to insulate perfectly. No avalanching is

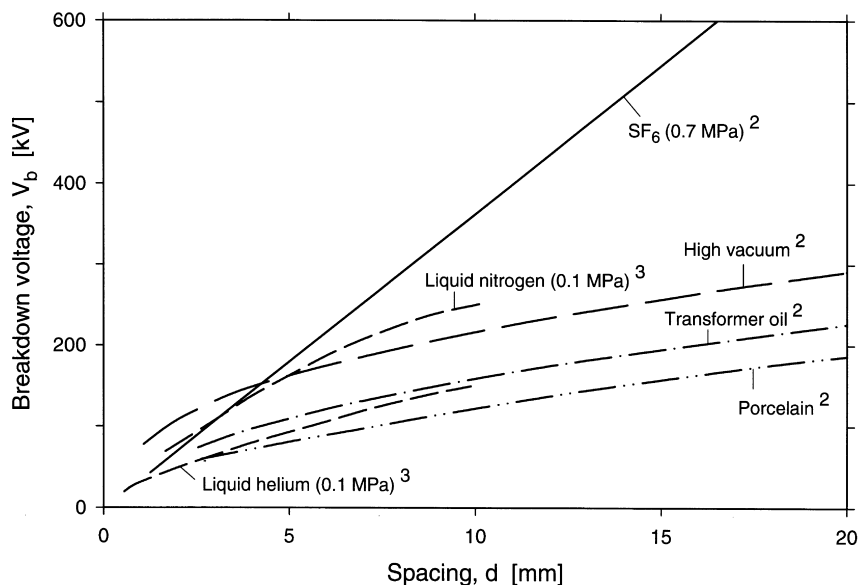


Figure 1 Breakdown strength of typical solid, cryogenic liquids, and vacuum insulation under d.c. voltage stress in a uniform field

possible within the stressed volume. However, electrons are emitted from a cathode surface at field strengths above some 10^7 V m^{-1} , which may equal 10^8 V m^{-1} at local surface protrusions. The prebreakdown current caused by electron moving across the gap with spacing d produces heat that must be removed by the refrigerator. At a sufficiently high emission level, breakdown becomes likely. This is due to the free fall of electrons through the gap voltage V before impinging on the anode. The high electron energy causes secondary emission effects. Surface conditions, therefore, are crucial for the performance of vacuum gaps. The very fast recovery, i.e. within nanoseconds, of a vacuum gap after breakdown should be especially emphasized⁷.

Prebreakdown current flow

Figure 2 illustrates the current flow across a planar vacuum gap with clean electrode surfaces vs stressing field strength E for various electrode materials and temperatures, respectively. The emission current density which depends on the cathode material and surface condition of course is considerably lowered at cryogenic temperatures^{8,9}. However, the amount of heat production per unit surface can easily come up to a level which is comparable to a.c. losses in a superconductor. These prebreakdown currents also define the amount of ‘dielectric losses’ in case of a.c. voltage stress. Electrode surface contamination, e.g. by adsorbate layers, can cause considerably higher prebreakdown currents, which may pulsate in a statistical manner¹⁰. Prebreakdown currents also may affect surface condition with time, i.e. cause either an improving or an impairing conditioning effect.

Breakdown

Increasing the stress results in an increasing current density. Secondary processes, e.g. photon and microparticle detachment^{2,6,7}, become more and more likely since the emitted electrons impinge on the anode with a kinetic energy according to the gap voltage $V = E \cdot d$. Careful conditioning may shift the breakdown voltage to higher levels, but this is not very reliable in practice; memory effects in vacuum

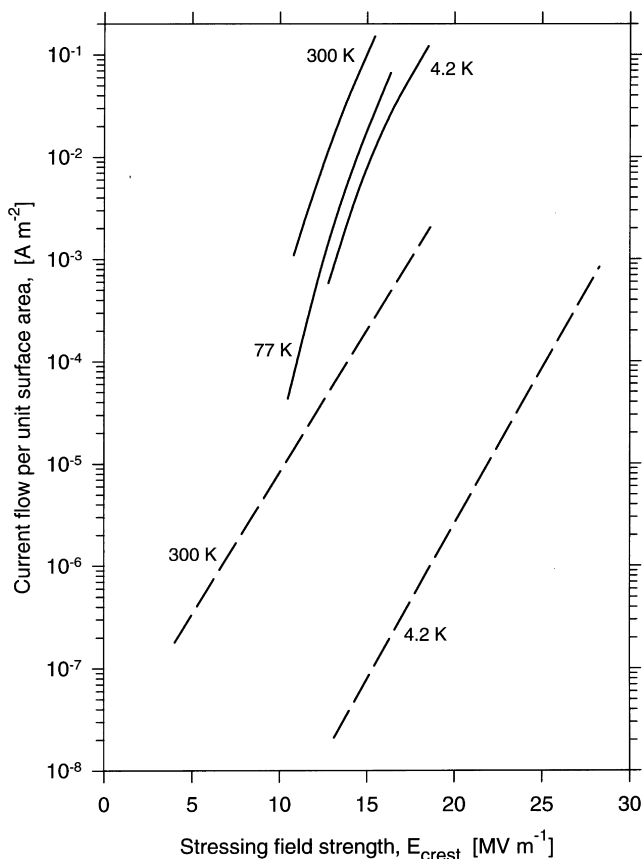


Figure 2 Predischarge current flow in a vacuum gap vs temperature. — copper electrodes, a.c. voltage⁸; - - - niobium electrodes, d.c. voltage⁹

gaps are indeed a very complex phenomenon^{11,12}. Breakdown is stress dominated at low spacing, but voltage dominated for large spacing². The breakdown voltage V_b in a uniform field gap rises approximately with the square root of the spacing¹³, i.e.

$$V_b = \sqrt{K \cdot d} \tag{1}$$

where the constant K depends on the actual electrode sur-

face condition, but also on the surface area A . The stored electrostatic energy being fed very rapidly into a beginning discharge has been claimed to be an important parameter. Hence $K \propto A^{-b}$, with b depending on the cathode material and surface state¹⁴. For low temperature gaps of laboratory size, e.g. planes of a few cm^2 area, K may range within 10^{12} and $10^{13} \text{ V}^2 \text{ m}^{-1}$ in case of short term d.c. and a.c. voltage breakdown. Non-uniform field gaps yield a total voltage effect, as can be seen in *Figure 3*¹⁵.

Impulse voltage stress may be even more adverse when no conditioning is being involved; considerably lower breakdown voltages than with d.c. or a.c. stress are the result¹¹. Degradation by adsorbed gas layers on a cold electrode surface, e.g. in case of a leak, can be dangerous and must be controlled. Statistical scattering of breakdown is an important fact with standard deviations as high as 25%, for instance^{11,16}; the particular probability distributions may be quite complex. Mixed distributions have been found in some cases, according to more than one distinct breakdown initiating mechanism. It may also be very difficult to maintain stable conditions in a vacuum gap over extended periods. Extrapolation to a very low breakdown probability in order to define a withstand level is not very straightforward, so high safety factors must be included in practice. Residual gas molecules, for instance, may be present in any practical vacuum system. Avalanching in an inadequate vacuum, for instance, caused by a helium leak, is the most critical kind of degradation in cryogenic vacuum systems; there is no stabilizing effect at all, and discharge paths become very

long with preference. Magnetic fields can have a very strong impact in addition, as can be seen in *Figure 4*; the trajectories of electrons are considerably elongated and ionizing collisions with residual molecules become more likely. This effect must be taken into account with superconducting magnets where very high magnetic fields are quite usual^{11,17}. *Figure 5* illustrates the breakdown course schematically.

According to all these adverse environmental conditions there is little chance to reliably withstand much more than 100 kV as a safe engineering limit in a single low temperature vacuum gap.

Cryogenic fluids

Helium and nitrogen are excellent insulating fluids for classical low critical temperature superconductors (LTS) and high critical temperature superconductors (HTS), respectively. Almost no problems with thermomechanical mismatch are involved. Many insulation systems in LTS applications are based on helium 4, either in its liquid state, in its supercritical state, or simply using the cold gas. Gaseous or liquid nitrogen, respectively, will be used in future HTS applications. Neon may eventually find some interest for HTS machines provided supply can be guaranteed at a reasonable price. Dielectric data for neon are scarce at present, and the performance can only be predicted in terms of analogy³.

All these fluids are self healing after discharge occurrence in so far as the respective atoms and molecules are chemically inactive. Moreover, a complete fluid exchange may often take place, e.g. in a cooling circuit where the fluid is completely reprocessed. Genuine fluid memory effects thus are not relevant in most applications, and no hazardous byproducts can be produced by discharges out of the fluid. However, a discharge may cause irreversible damage to adjacent electrodes and solid insulators, respectively.

Current flow

The fluids are normally free from charge carriers. Leakage currents can be caused only by ionizing radiation, which may be reduced inside a cryostat. Non self-maintained discharge current densities are below 10^{-9} A m^{-2} . Extremely high resistivity values have been found in the liquids, e.g. $> 10^{16} \Omega \text{ m}^{-1}$ in liquid helium. Leakage currents are often not detectable unless charge carriers are emitted from the electrodes; this needs a high local field strength of more than 10^8 V m^{-1} .

Permittivity

The molecules of cryogenic fluids are non-polar. The Clausius-Mosotti formula can be used in order to evaluate the relative permittivity ϵ_r for any particular thermodynamic state³. Data for the molecular polarizability to the permittivity of space ratio, $\alpha_i/3\epsilon_0$, which does not depend on the fluid state, are indicated in *Table 1*. Relative permittivities in the gaseous state are very close to unity. In the liquid state, however, the fluid density number becomes extremely large. There is a strong correlation between the liquid permittivity ϵ_{rL} and the normal boiling temperature T_{nbp} ; this is because the internal Van der Waals forces which are

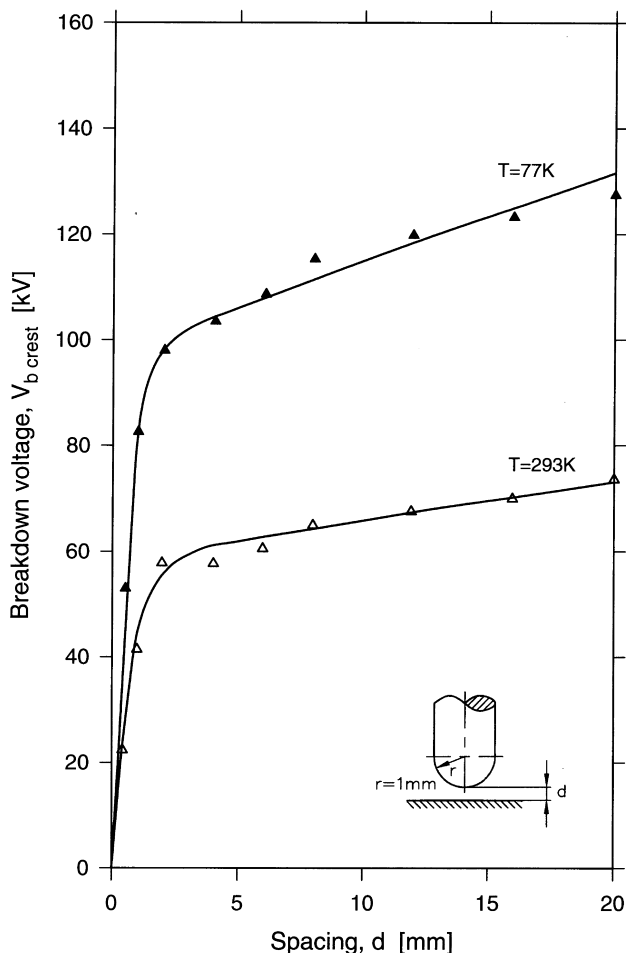


Figure 3 Breakdown in a non-uniform field vacuum gap; a.c. voltage with copper electrodes

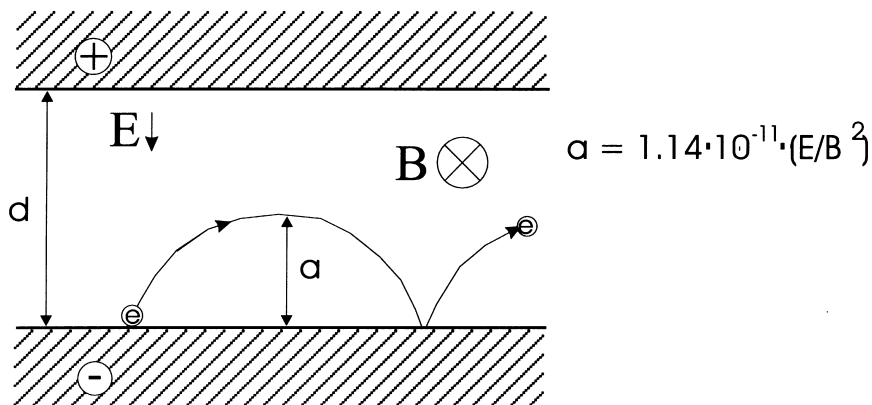


Figure 4 Electron motion in uniform electric field E in a perpendicular magnetic field B

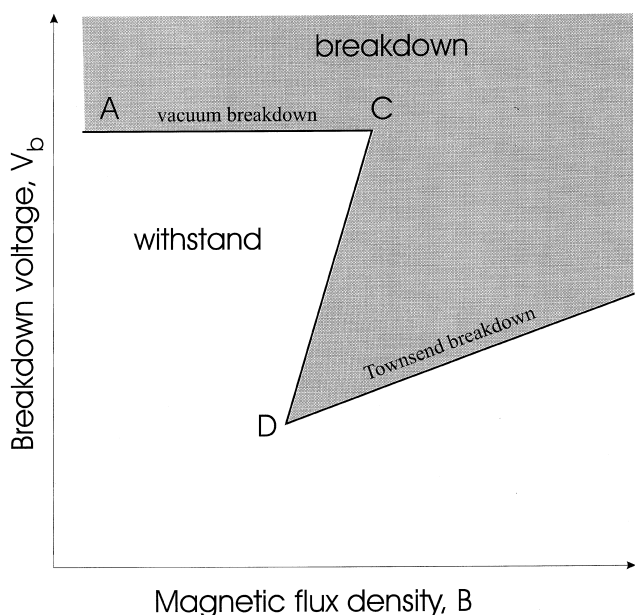


Figure 5 Conceptual characteristics of vacuum breakdown voltage vs magnetic field

Table 1 Polarizability and permittivity of crogenic fluids

Fluid	$\alpha_i/3\epsilon_0$ (m^3)	ϵ_{rL}	T_{nbp} (K)
Helium	$8.6 \cdot 10^{-31}$	1.05	4.2
Neon	$16 \cdot 10^{-31}$	1.19	27.2
Nitrogen	$72.5 \cdot 10^{-31}$	1.44	77.3

responsible for condensation are due to fluctuating dipole moments³. This also can be seen in *Table 1*. The permittivity is an almost ideal intrinsic fluid parameter.

Liquids may be inhomogeneous when bubbles are present. Any stressing electrical field is enhanced within the bubble from its bulk value by an order of $\epsilon_{rL}/1$. This effect must be born in mind, especially since vaporization is easy in cryogenic liquids. A moderate field distortion also is caused by frozen foreign gas particles. Accommodation with solids is difficult due to the much higher permittivity of the latter, i.e. two up to more than five. Thus, solid contaminants such as dust particles can result in a serious local field enhancement. These particles are pulled to high stress points by dielectrophoretic forces, and can initiate discharges there.

Dielectric losses

Dielectric losses may be expected to be extremely low at power frequencies. Dielectric absorption is not relevant then. In fact, no losses could ever be found in any cold gas. However, surprisingly high losses have been measured in the liquids, even at power frequencies. *Figure 6* gives a survey about the loss order of magnitude in liquid nitrogen and liquid helium, respectively^{18,19}. Losses have been found to vary with time. The loss level cannot be taken as an intrinsic liquid property thus. Predischarges have been claimed sometimes to be the origin of losses, but these can be excluded definitely in liquid nitrogen for instance. The

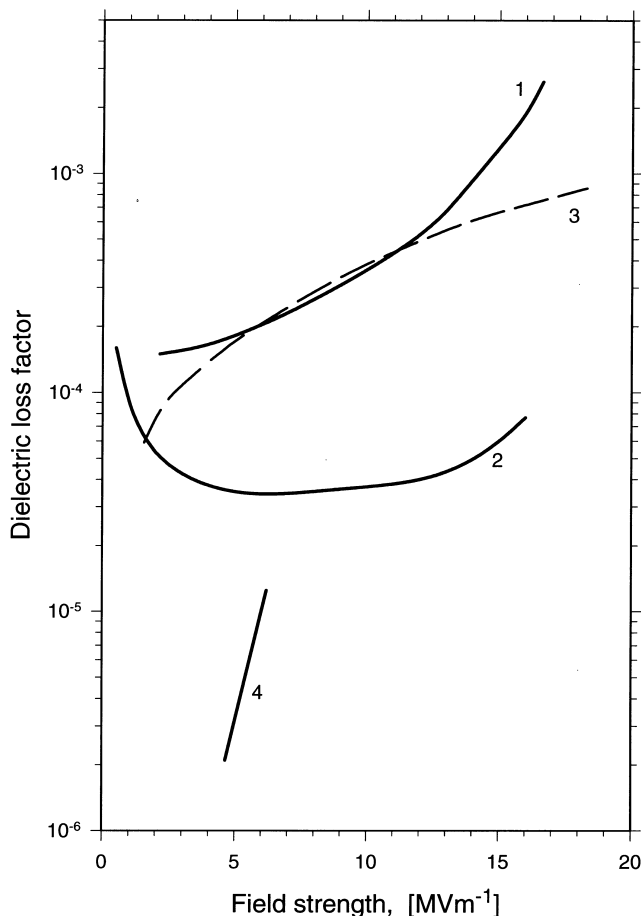


Figure 6 Dielectric losses in liquids near the normal boiling point at power frequency: 1, 2, 3 = liquid nitrogen¹⁸; 4 = liquid helium¹⁹

most probable loss source may be foreign impurity particles, or electrode-adjacent phenomena which show a distinct memory effect¹⁸. However, the liquid nitrogen loss level ranging in between curve 1 and 2, for instance, may be quite compatible with the needs for a low loss dielectric system at 80 K operating temperature.

Dielectric strength

Discharge onset begins when the rate at which free electrons are produced exceeds the rate of removing them substantially. An exponentially growing avalanche up to a conducting path, i.e. a streamer, then is formed which finally may turn into an arc. Such a catastrophic event has to be prevented safely by a proper design.

Gas breakdown

Breakdown in uncontaminated gases at a not too high stress is a near-intrinsic function of the gas state. Figure 7 shows the nitrogen Paschen curve, i.e. the breakdown voltage V_b versus the density number times spacing product $N_v \cdot d$ ^{20,21}. Scattering right of the Paschen minimum and in the far breakdown region right of it is extremely low, and no size effect normally is involved. The Paschen curve for neon as a monatomic noble gas is included for comparison³; a distinct shift against the nitrogen Paschen curve is obvious. The former wide scattering range of helium gas breakdown²¹ has been considerably confined for the far right region down to the Paschen minimum by very careful new experiments²², see Figure 8.

The formative breakdown time lags may range below 1 μs ²⁰. The excess of pulse breakdown over the static breakdown voltage, which is a statistical phenomenon in time since there is a statistical time lag, is utilized with benefit in air via the so called impulse factor in the statistical design method. However, superconducting apparatus should be designed by the definite design method¹. Hence the breakdown probability must be close to zero, and no impulse factor related to the statistical time lag should be used.

To break down a gas, the stressing field E must intersect a critical number of gas molecules. Electron multiplication

along the gap length d must reach a critical amount k of the order of unity in helium, and of 10^7 in nitrogen, respectively. Breakdown initiation thus can be formulated as²³

$$\exp\left\{\int_{x=0}^d \alpha[x] \cdot dx\right\} = k \tag{2}$$

where $\alpha[x]$ is the first Townsend ionization coefficient; it depends strongly on the field strength course $E[x]$ within the gap. None of the cryogenic gases is electron attaching. This simple equation relates to the far right part of the Paschen curve. The gas temperature has practically no influence on breakdown^{24,25}. The amount of impact ionization α is correlated with the density number and the ionization voltage of the particular gas. This can be written as $\alpha \cdot N_v^{-1} = f\{V_i, E \cdot N_v^{-1}\}$. Figure 9 indicates the respective characteristics.

Uniform field breakdown. Equation (2) reads simply $\exp(\alpha \cdot d) = k$ in a uniform field where $E = \text{constant}$ across the gap. This implies a constant α -value. The general Paschen law claims that the breakdown voltage V_b , is a pure and monovalent function of the density number times spacing product, $N_v \cdot d$, for any particular gas²¹. Hence

$$V_b = f\{N_v \cdot d\} \tag{3}$$

This has already been illustrated in Figures 7 and 8. Helium and neon as monatomic noble gases are the weakest of all gaseous insulators at a corresponding density number, and the relative electrical strength (RES) at ambient conditions of helium (RES = 1/12) and neon (RES = 1/4) is low in comparison with air. Nitrogen gas on the other hand shows an RES of almost unity^{21,26}. The correctness of Equation (3) in the cryogenic temperature domain has been confirmed experimentally in nitrogen and helium, respectively, by many workers in the field. Cooling down to the saturated vapour density yields a quite similar vapour strength for nitrogen and helium far right of the Paschen minimum, see Figure 10. The different amount in concentration is almost offset by the different ionization amount²⁴.

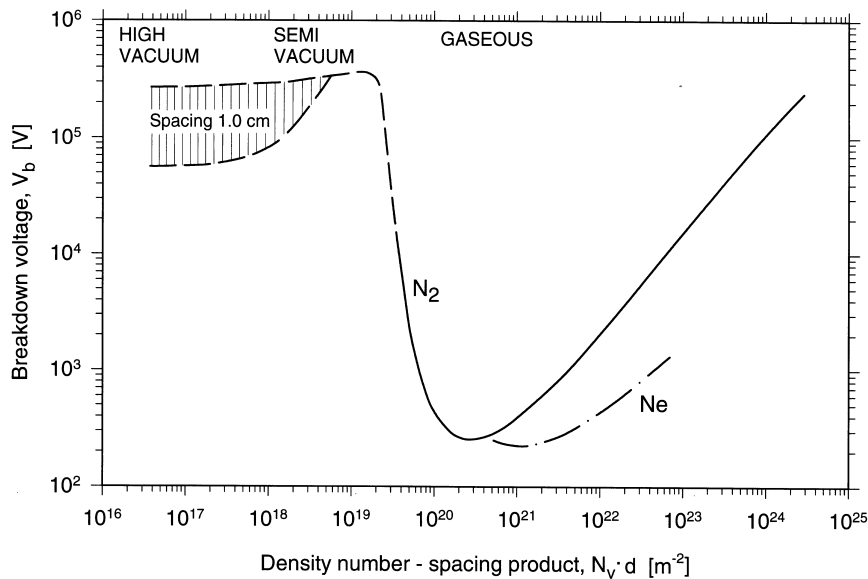


Figure 7 Paschen curve for nitrogen and neon

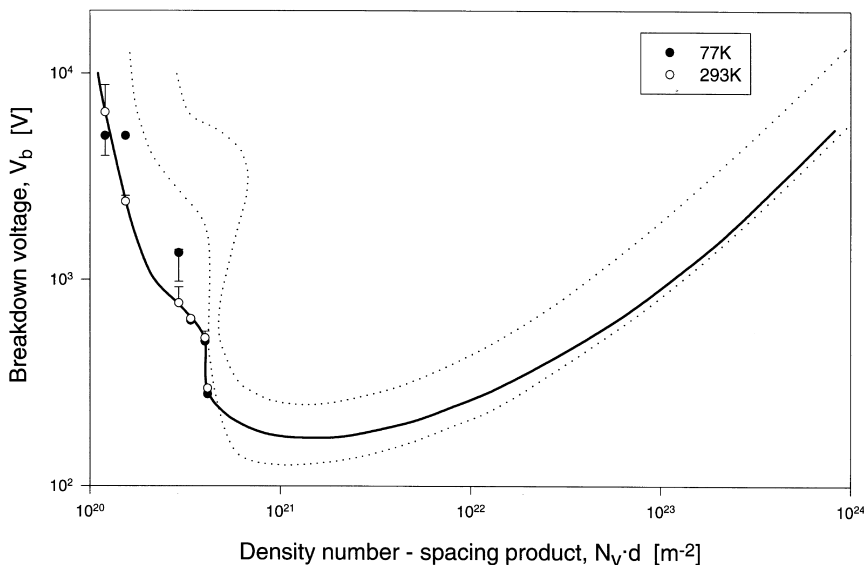


Figure 8 Paschen curve for⁴ helium. --- boundaries of CIGRE Paschen curve scattering; — fit curve for ambient temperature and low temperature data; ● discharges in semivacuum at low temperature; ○ discharges in semivacuum at ambient temperature

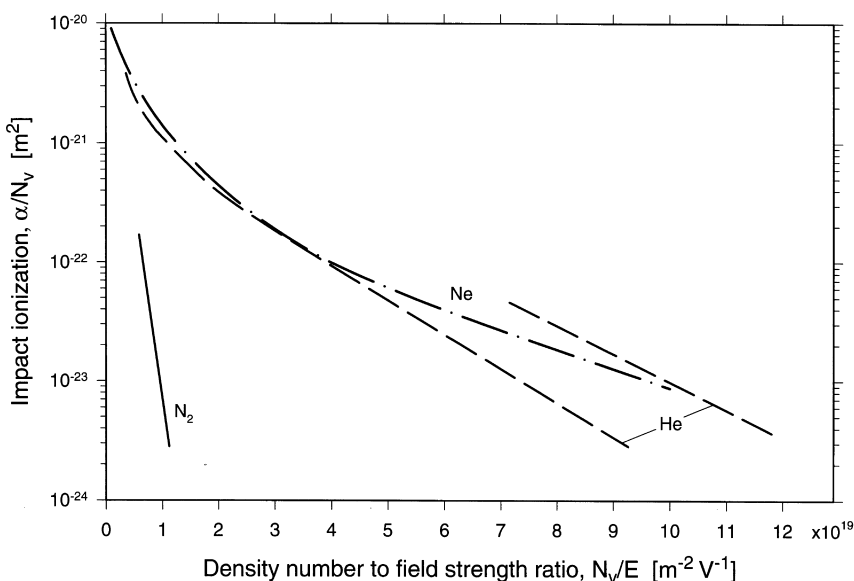


Figure 9 Impact ionization, α/N_v , vs the density number to field strength ratio, N_v/E , in nitrogen, neon, and helium gas

Hence, a cold vapour will show a reasonable dielectric strength. Neon may be not so a favourable candidate for cryogenic dielectric insulation, since its extrapolated vapour strength remains considerably below the nitrogen and helium level. No experimental low temperature breakdown data, however, are known for neon gas.

Breakdown voltages remain below the Paschen level if the field strength at the cathode exceeds 10^7 V m^{-1} . This is typical for high gas densities which come out automatically when cooling down a pressurized gas to low temperature. Additional electron emission or micro-gas discharges may be responsible²¹. The effect is well known in various gases at ambient temperature. *Figure 11* shows the general trend in cold helium gas. Breakdown then is not an intrinsic gas parameter at high stress. Increasing statistical scattering also must be encountered. Of course, actual electrode surface quality becomes an important an extrinsic parameter.

A significant breakdown voltage reincrease occurs for very low density numbers in the near breakdown domain, i.e. left of the Paschen minimum where the electrons cannot

be ‘thermalized’. This regime provides a steady transition to vacuum breakdown; it is called a ‘semivacuum’ now and then, as having already been indicated in *Figure 7*. It must be pointed out that any transition from vacuum via the far left Paschen curve, e.g. in cases of a leak into a voltage stressed vacuum space, has been claimed to become a dangerous scenario for superconducting magnets. The breakdown then follows with preference the largest discharge path within the stressed vacuum chamber; any prediction of a withstand voltage may be arbitrary^{22,27}. Experiments in this domain normally reveal a very large scattering of data; the semivacuum range should be avoided in any practical insulation system. Strong magnetic fields may shift the low Paschen minimum voltage region considerably to the left¹ unless special geometrical configurations are used¹⁷.

Non-uniform field discharges. Discharges in a strongly non-uniform field must not end directly in breakdown, but often yield a stable current flow, i.e. a corona.

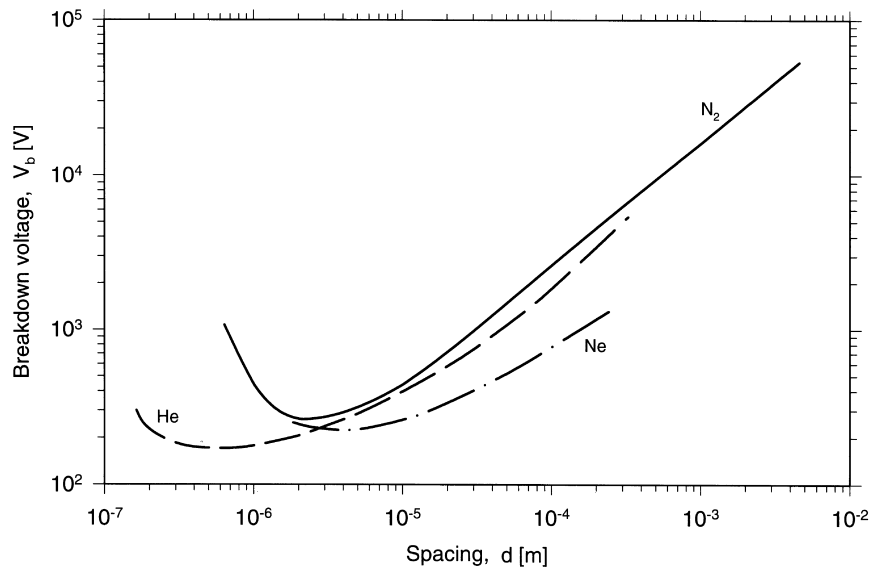


Figure 10 Breakdown voltage, V_b , vs spacing in nitrogen, neon, and helium vapour close to the normal boiling point

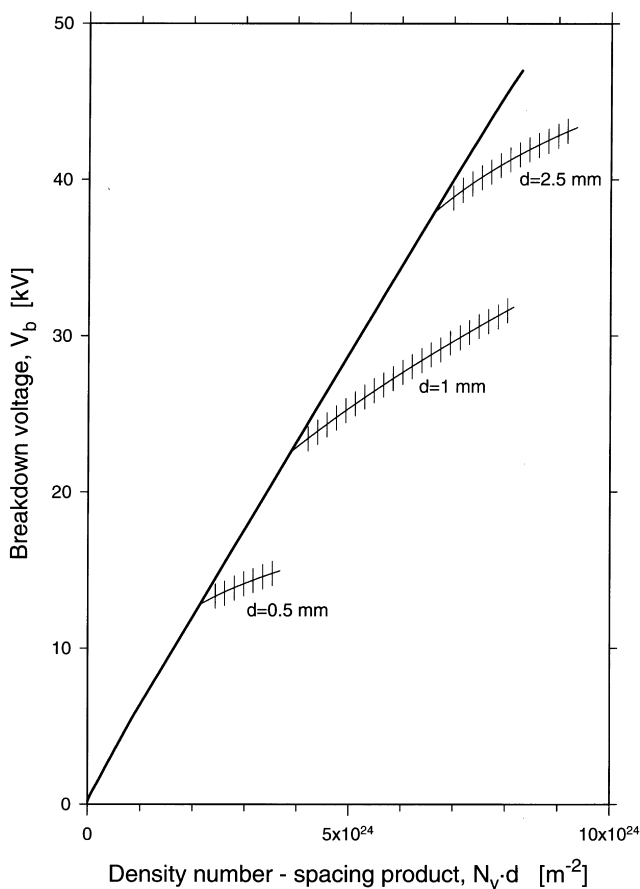


Figure 11 High stress breakdown in cold helium gas. — Paschen curve; +++ high stress breakdown at constant spacing

High stress points normally are shielded by ions which form a space charge at a not too low density number. Nitrogen, neon and helium are non-attaching gases, i.e. electrons cannot be caught easily by the molecules. However, negative ions of limited lifetime can occur, and negative ion clouds can shield high stress regions in a non-uniform gap, for instance a point electrode. Helium on the other hand builds up no negative ions at all, and negative space charge shielding normally is impossible.

The current flow caused by ion moving produces corona losses which heat up the stressed gas and decrease the local gas density; gas thinning may be moderate at ambient temperature since heat diffusion is very effective. Thinning of the surrounding gas is much more severe at low temperatures since heat diffusion is weak, and the corona losses must be cooled by a refrigerator. Thus, corona must be eliminated in normal operation; it may be tolerable to some extent, i.e. with a safe limit against breakdown, in case of transient overvoltages, or in case of a quench in a superconducting apparatus. Corona onset can be calculated in general from Equation (2) with the ionization parameter $\alpha\{x\}$ found in accordance to the local field strength course $E\{x\}$; k may be derived from uniform field breakdown data. *Figure 12* illustrates measured divergent field corona and breakdown in cold helium gas, and *Figure 13* in gas nitrogen gas, respectively^{23,28}. A higher gas density leads to higher voltages. However, corona onset voltages V_c often show a distinct saturation for larger gap lengths. The breakdown voltages increase regularly with gap length when the point is positive. In case of a negative point, a delayed increase is found in a near-saturated vapour. This effect may be attributed to electron trapping. Little is known about low temperature breakdown statistics.

Liquid breakdown

The dielectric strength of liquids is never a pure materials function. Any 'intrinsic strength' is fictitious in the strong sense. However, it can be taken as a kind of asymptotic approximation. Breakdown or discharge voltages can only be measured as a function of the overall electrode/liquid system; extrinsic parameters have an important effect, and statistical scattering can be considerable. These phenomena are quite similar to any other insulating liquid²⁹.

Quoted strength. The quoted breakdown strength E_b , usually is defined by the almost uniform field breakdown voltage to gap length ratio, V_b/d . Very high quoted breakdown fields (d.c. or a.c. voltage) of the order of 40–100 MV/m in non-boiling liquid helium, and 70 up to > 200 MV/m in non-boiling liquid nitrogen, have been claimed in the mid seventies to be typical under well controlled

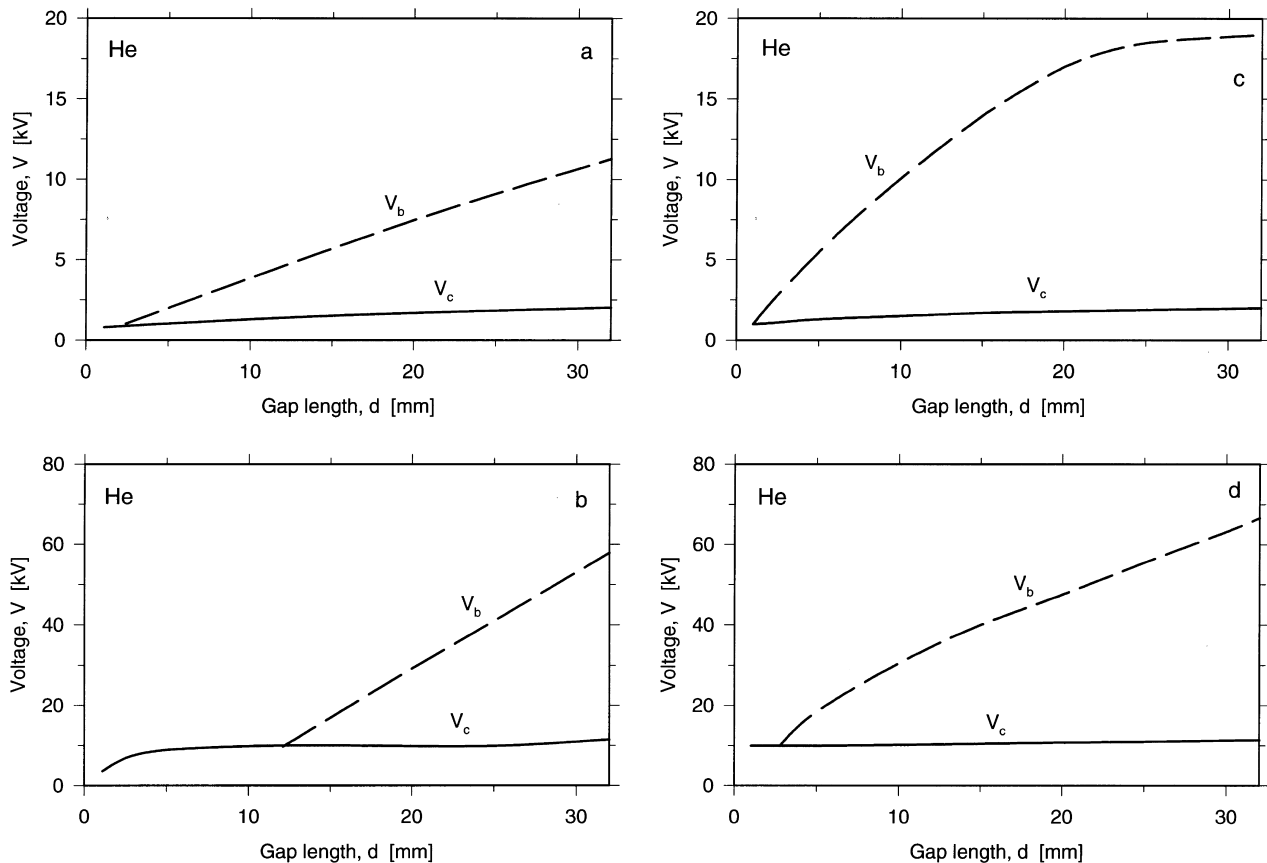


Figure 12 Corona onset voltage, V_c , and sparking voltage, V_b , in a point to plane gap; gaseous helium. (a) $N_v = 2.0 \cdot 10^{26} \text{ m}^{-3}$ at 40 K; point negative. (b) $N_v = 2.7 \cdot 10^{27} \text{ m}^{-3}$ at 4.2 K; point negative. (c) $N_v = 2.0 \cdot 10^{26} \text{ m}^{-3}$ at 40 K; point positive. (d) $N_v = 2.7 \cdot 10^{27} \text{ m}^{-3}$ at 4.2 K; point positive

laboratory conditions^{29,33}. Liquid neon data are very scarce; a quite similar strength of almost 70 MV/m has been measured at 100 μm spacing, however³⁰. All these high strength values can only be found as short term breakdown at low spacing and with small-scaled polished electrodes. Any severe degradation has to be prevented in order to guarantee a high strength level at d.c. or a.c. stress: careful filtering out of field distorting particles should be provided for instance. The liquids must not be accepted with the arbitrary ‘technical purity’ from the supplier. However, the quoted strength takes no account for any size effect, i.e. the stressed liquid volume and stressed electrode area, respectively. The stressing time also can have a significant influence.

Commercial liquids. A pure liquid without any degradation may be a fiction in practical applications. Breakdown under technical conditions is weak-link dominated in a statistical sense. Near-uniform field short term breakdown voltages close to the normal boiling point may be estimated from³¹

$$V_b = C \cdot d^{0.8} \tag{4}$$

where $C = 21.5 \text{ kV mm}^{-0.8}$ for ‘technical grade’ liquid helium, and $29 \text{ kV mm}^{-0.8}$ for ‘technical grade’ liquid nitrogen, respectively. This engineering formula relates to the statistical mean breakdown voltage and indicates only orders of magnitude.

Size effect. The inherent size effect must be taken into account. Increasing the stressed size, i.e. the number of

stressed unit cells, increases the probability for the occurrence of active sites for streamer initiation. A quite simple engineering order of magnitude estimation may rely onto^{31,35–37}

$$E_{b1} = E_{b2} \cdot \left(\frac{S_1}{S_2} \right)^{-1/m} \tag{5}$$

(E_{b1} : mean breakdown field strength with stressed size S_1 , i.e. N_1 stressed unit cells; E_{b2} : mean breakdown field strength with stressed size S_2 , i.e. N_2 stressed unit cells). The exponent $1/m$ can be evaluated from the experimentally found relative standard deviation s_r , according to Weibull³⁵, see Figure 14. Standard deviations up to 20% have been found often, but less than 10% may be taken as an upper limit in larger gap systems. The occurrence of a size effect must be anticipated, according to many experimental findings.

Prediction of the size effect by means of statistical data from small scaled experiments seems to be enticing. A detailed statistical evaluation could be carried out recently for short term liquid helium breakdown³⁷. The total gap voltage in a moderately non-uniform field gap configuration as given by the field strength course $E(x)$, i.e. $V = \int_0^d E(x) dx$, causes a maximum breakdown stress E_b at the electrode surface. This allowable maximum stress is related to the stressed size via Equation (5); a stressed region where the field strength exceeds $\approx 80\%$ of the nominal field strength E_b seems to be relevant. Unfortunately, no distinct correlation between statistics and size effect could

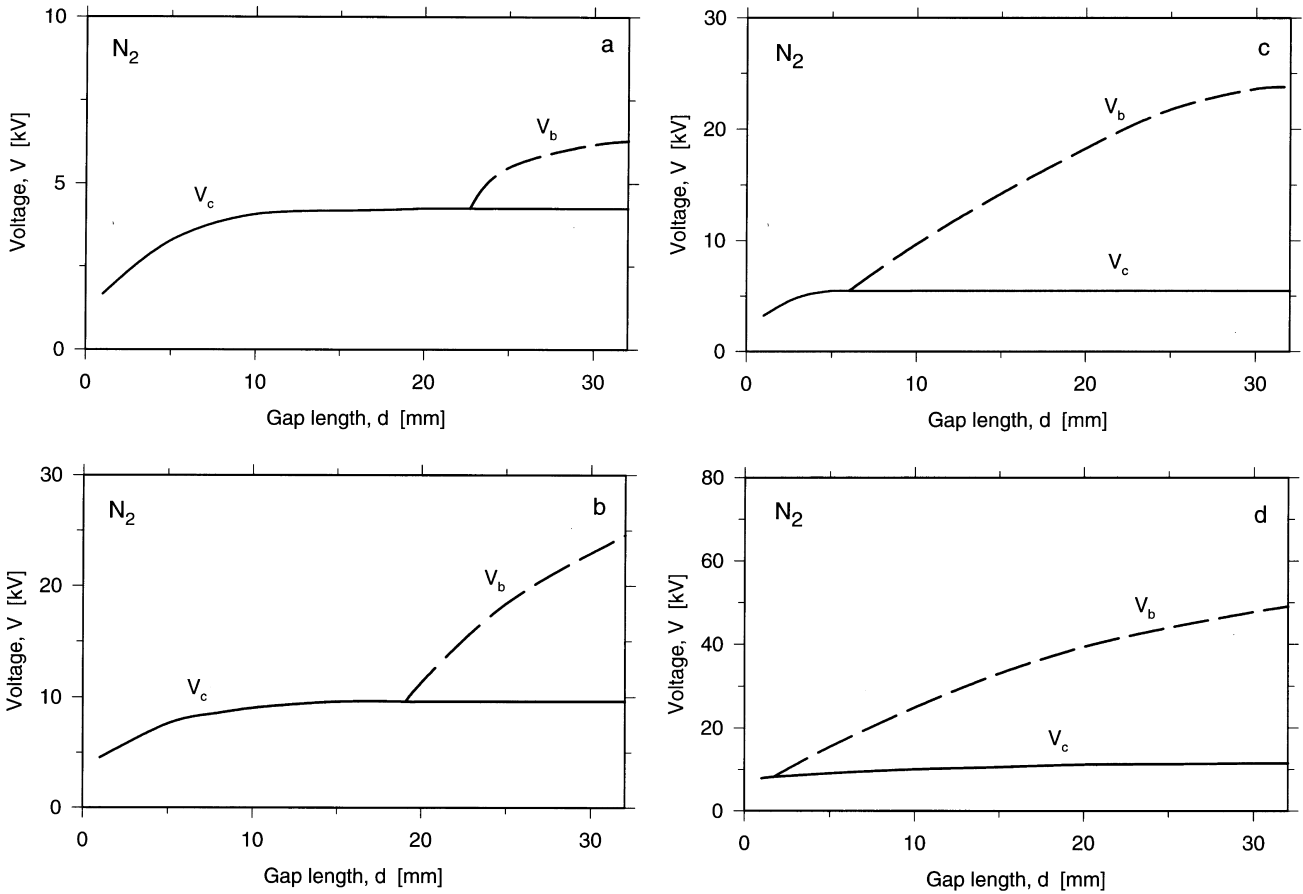


Figure 13 Corona onset voltage, V_c , and sparking voltage, V_b , in a point to plane gap; gaseous nitrogen at 78 K. (a) $N_v = 2.3 \cdot 10^{25} \text{ m}^{-3}$; point negative. (b) $N_v = 9.1 \cdot 10^{25} \text{ m}^{-3}$; point negative. (c) $N_v = 2.3 \cdot 10^{25} \text{ m}^{-3}$; point positive. (d) $N_v = 9.1 \cdot 10^{25} \text{ m}^{-3}$; point positive

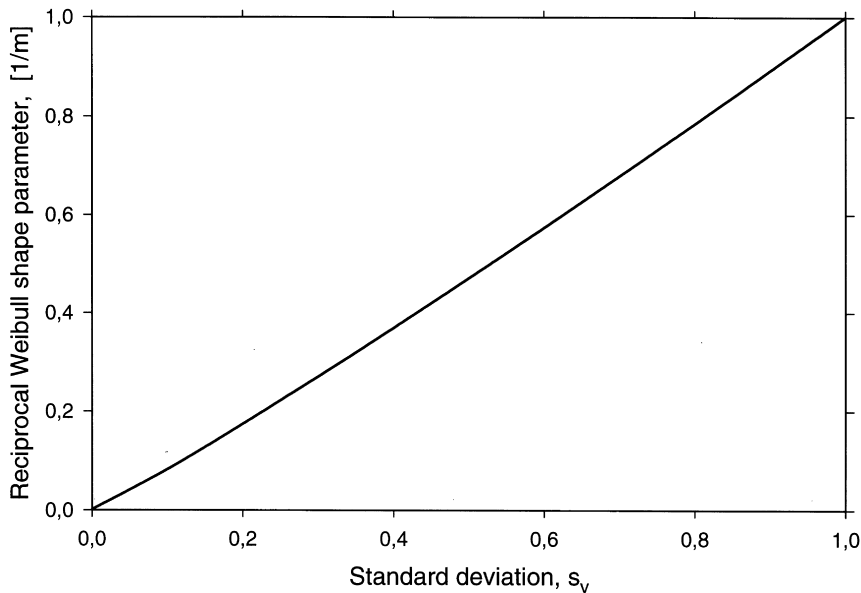


Figure 14 Size effect parameter, $1/m$, vs relative standard deviation, s_v

be defined in case of d.c. or a.c. stress, respectively. However, the occurrence of a genuine area effect has been made obvious in case of μs pulse voltage stress in liquid helium. This area effect coincides well with the fitted Weibull probability distribution³⁸. It seems that no activation of initiating sites in the bulk liquid can take place in a very short time.

Data for short term a.c. voltage breakdown in ‘technical grade’ liquid nitrogen are somewhat non-uniform. Standard

deviations of the order of 10–25% have been communicated in small sized gaps³⁹; the mean breakdown stress being surprisingly low, i.e. 11 kV/mm (rms), which may be partly due to vapour bubble occurrence in the stressed region. Lower standard deviations of the order of 11% on the other hand have been measured at the normal boiling point with a mean breakdown stress of 20 kV/mm at 50 cm^2 stressed area, but only 7% at 0.2 MPa pressure with

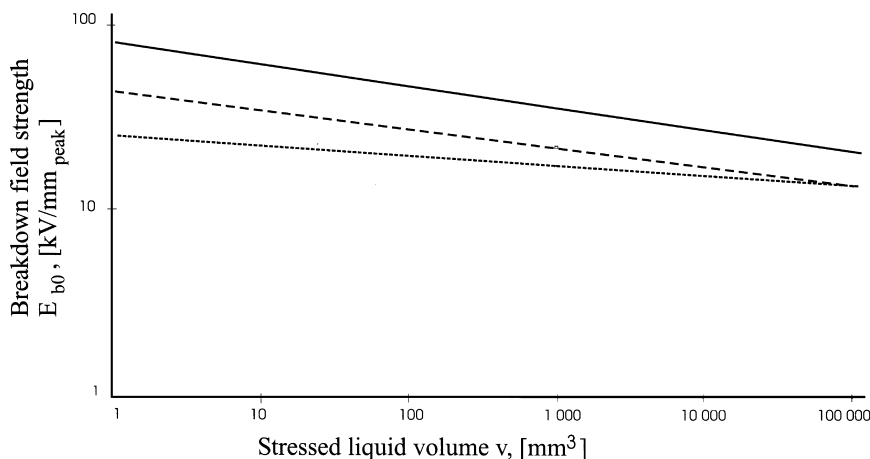


Figure 15 Volume effect in liquid helium breakdown. — fit from ref. ³⁶; --- data from ref. ³¹; ... near zero breakdown probability estimation from ref. ³⁷

45 kV/mm⁴⁰; the related exponent $1/m$ in Equation (5) then may be of an order of 0.1 and 0.05, respectively. A larger standard deviation of $\approx 20\%$ has been found in some other experiments carried out in a normal boiling liquid nitrogen filled coaxial gap of 1 mm spacing and almost 80 cm² stressed area; the mean rms breakdown voltage then was of the order of 20 kV⁴¹. These data suggest a surprisingly large exponent $1/m$ close to 0.2. More recent breakdown experiments in boiling liquid nitrogen finally yielded a $1/m$ figure decreasing with size from 0.1 down to 0.07 for an average rms breakdown strength ranging in between 17 down to 12 kV/mm⁴².

However, there may be some general objection against a statistical evaluation of the size effect. Any experimental breakdown statistics can only overlap a limited probability interval of course; test expenditure would be excessive otherwise. The usual fitting procedures—although often very sophisticated—can give no proof that the evaluated probability function is the full truth at all; all fits yield a most likely approximation. Thus, a more satisfying engineering approach may be to rely onto directly measured size effect characteristics. *Figure 15* indicates d.c. breakdown in liquid helium vs the stressed volume v as the relevant

size parameter; the volume was claimed to result in a better approximation to experimental data in non-boiling liquid than the stressed electrode area³⁶. The volume effect exponent $1/m$ in Equation (5) was found close to 0.1; a very similar figure covers breakdown data in supercritical helium³⁶, and also fits well to a.c. breakdown data³¹. There may be a parallel shift of stress downwards to 1/3 in case of adverse cathode conditions, e.g. surface roughness $> 10 \mu\text{m}$ ^{32,34}. Extremely low d.c. voltage breakdown values which are hard to believe in have been communicated recently for liquid helium⁴³. However, no electrode surface specification is specified.

A somewhat higher volume effect slope with $1/m \approx 0.14$ for a.c. voltage breakdown in saturated liquid nitrogen has been communicated in Okubo *et al.*³¹. This figure is within the range having already been estimated from the data in other work^{39–41}.

Some authors still insist that the stressed electrode area is the breakdown controlling parameter instead of the stressed volume^{38,40,44}. Although this idea may be correct in uncontaminated liquids under well controlled experimental conditions, it neglects any direct spacing effect; the latter is commonly accepted in insulating liquids. The spacing

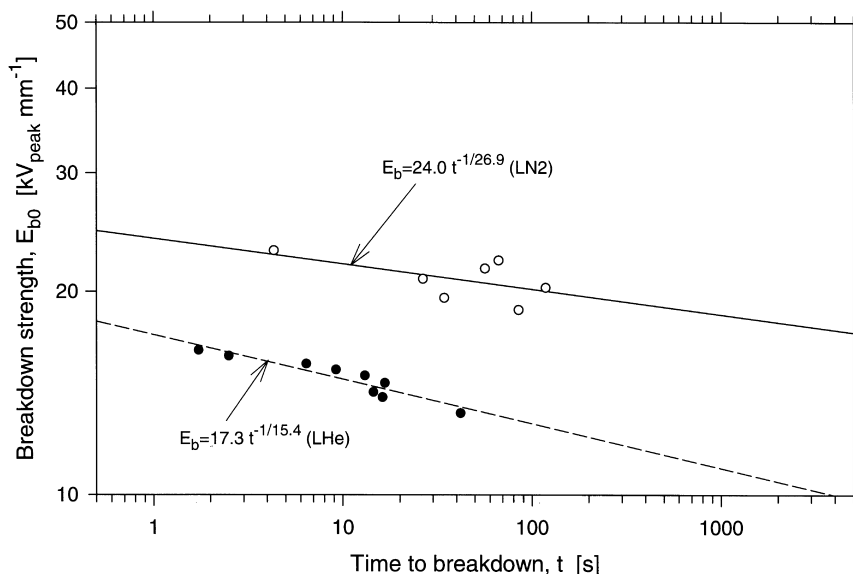


Figure 16 Breakdown strength–time characteristics at power frequency in a coaxial cylindrical electrode system; spacing 4.5 mm, cylinder \varnothing 42.5 mm, cylinder length 100 mm

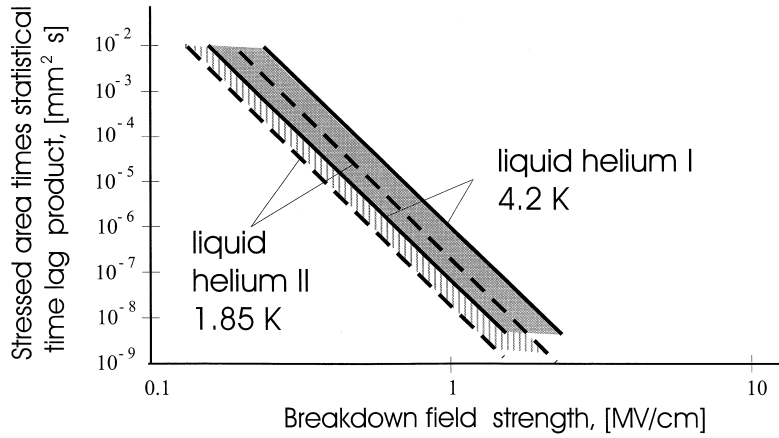


Figure 17 Mutual interference of breakdown field strength and statistical time lag in near-saturated liquid helium

effect can be understood by interference with the stressed liquid volume. A mutual interaction of area and volume effect, respectively, may be the most probable overall mechanism. It has been made obvious in a.c. voltage breakdown of boiling liquid nitrogen⁴⁵. Breakdown then was partly attributed to bubbles occurring within the stressed gap.

Great caution must be applied in general when making any extrapolation out of the range being directly covered by experiments in order to define a withstand voltage in the definite design method, according to all these uncertainties. A near-zero breakdown probability must be estimated for the definite design method. In non-boiling liquid helium with smooth electrodes for instance, a volume effect characteristics with $1/m \approx 0.05$ has been recommended recently³⁷; this almost zero breakdown probability seems in fact to remain below almost any known breakdown data. The corresponding characteristics is indicated in Figure 15. A competing evaluation for liquid nitrogen should be carried out very soon, in order to meet the needs for designing future HTS system insulation.

Long term degradation. Weak link activation also is a time dependent phenomenon. In fact, liquid breakdown

cannot be given in terms of gap configuration and stressed size without referring to the stressing time t ⁴⁶. Only few medium term (up to one hour) a.c. breakdown data in normal boiling liquid helium and liquid nitrogen, respectively, are available and can give an impression about the possible tendency. These characteristics are shown in Figure 16³¹, and suggest the usual life equation⁴⁶

$$E_b\{t\} \cdot t^{1/n} = \text{const} \tan t \tag{6}$$

Whether the long term degradation is due to any memory effects of the electrode-liquid system, or is merely a statistical phenomenon, cannot be decided yet. In any way, chemical reactions on electrode surfaces may occur¹⁸.

Very limited information about the simultaneous degradation in size and stressing time is known. Pulse voltage breakdown experiments in the μs range, both in normal boiling liquid helium I³⁸ and saturated superfluid helium II⁴⁴, revealed no memory effect at all; the data fairly well fitting into Laue plots⁴⁶. Some idea about the mutual interaction can be get from Figure 17. The breakdown field strength depends on the stressed area times the mean statistical time lag, which can be explained in a consistent manner by means of the probability for the occurrence of initiat-

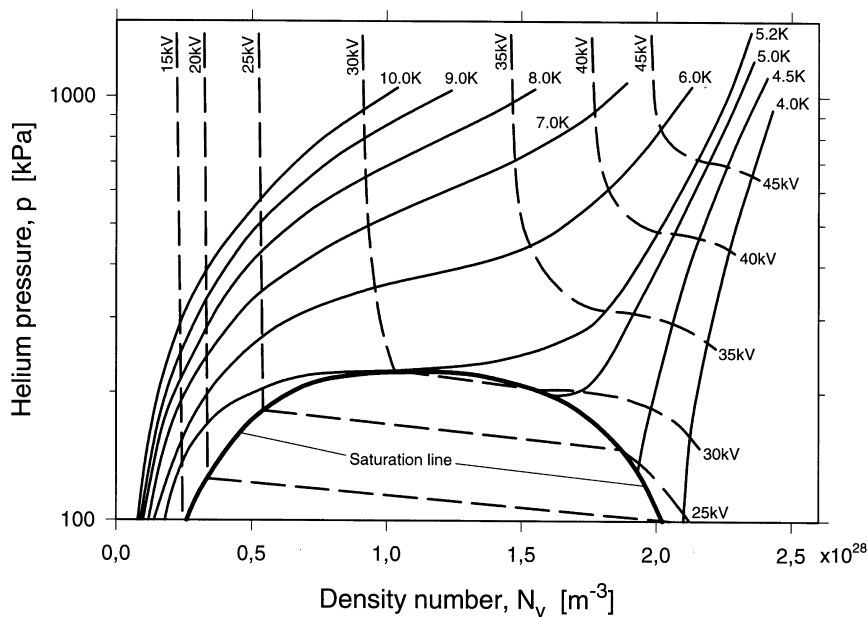


Figure 18 Contour plot of uniform field d.c. breakdown voltages in helium; 1 mm gap, stressed area 28 cm²

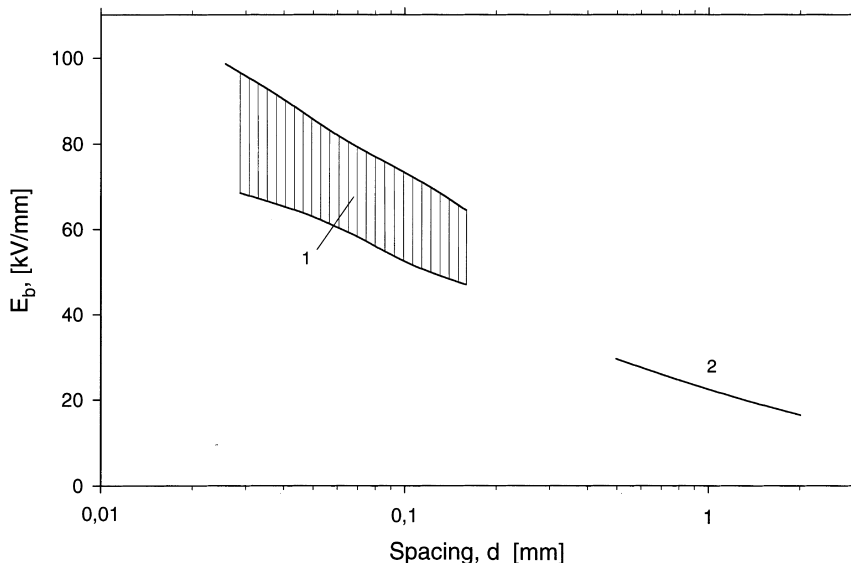


Figure 19 Uniform field d.c. breakdown strength of saturated LHe II near 2.0 K vs spacing. (1) dia. 25 mm stainless steel spheres⁴⁵; (2) \varnothing 9.5 mm aluminum sphere-to-stainless steel plane⁴⁹

ing electron emission from the cathode. The data may be used to evaluate the withstand voltage in a particular gap configuration by introducing the pulse duration as the relevant time lag. The pulse withstand voltages are considerably higher compared to the corresponding d.c. or a.c. voltage level. An appropriate safety margin must be incorporated however: the statistical time lags are grouped around the mean time lag following a Weibull distribution function. An almost zero breakdown probability only comes out when the pulse duration is below the formative time lag of course.

Pressurized liquids. Liquid pressure allows a wide variation of thermodynamic states, and has a strong impact on breakdown. The steady transition from gas breakdown to liquid and supercritical liquid breakdown has especially been investigated in gaseous, liquid and supercritical helium, due to practical needs for data, but also since these states could be easily maintained in the experiments³⁴. *Figure 18* shows an iso-breakdown voltage diagram versus helium pressure and density number, which has originally

presented by Meats⁴⁷ for carefully controlled experimental conditions. However, liquid helium II has become of special interest due to its fascinating cooling performance. The near-saturated liquid can be assumed with a uniform field breakdown strength in the liquid helium I range^{34,44,48,49}, as can be seen in *Figure 19*; the saturated vapour bubble strength however may be lower by an order of magnitude³⁴. A high pressure can yield a considerable higher strength: up to two times the strength as being indicated in *Figure 19* has been found at 0.1 MPa for instance⁴⁴. Considerably lower pressurized LHe II breakdown values, i.e. an order of only 10 kV/mm at almost ambient pressure, have been communicated in reference⁴³.

There is no corresponding diagram for liquid nitrogen, but the general trend of the near uniform field breakdown strength increase with increasing pressure p is illustrated in *Figure 20*⁴⁵. A kind of saturation can be observed. Of special interest may be the initial slope of the relative breakdown field strength against the pressure rise $\partial\left(\frac{E_b\{p\}}{E_b\{0.1\text{ MPa}\}}\right)/\partial p$ just around 0.1 MPa, versus the

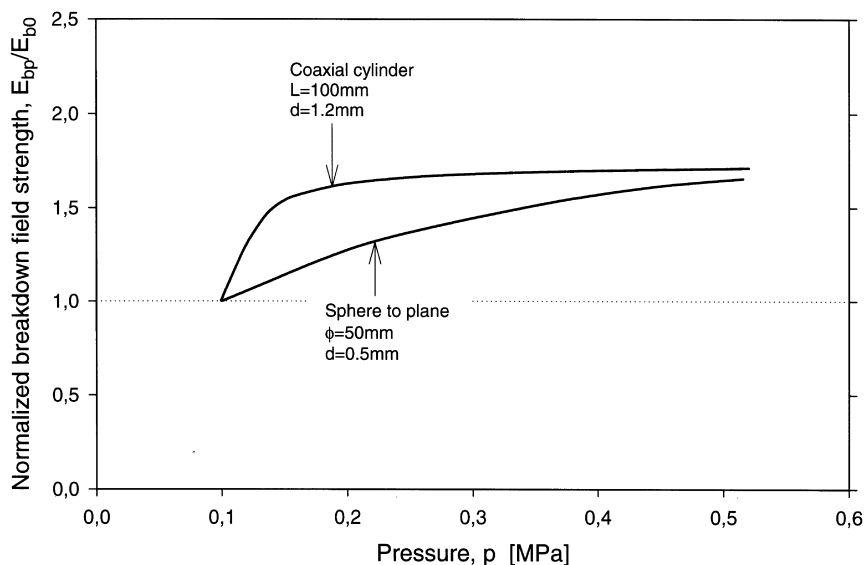


Figure 20 Normalized breakdown strength, E_{bp}/E_{b0} , vs liquid nitrogen pressure

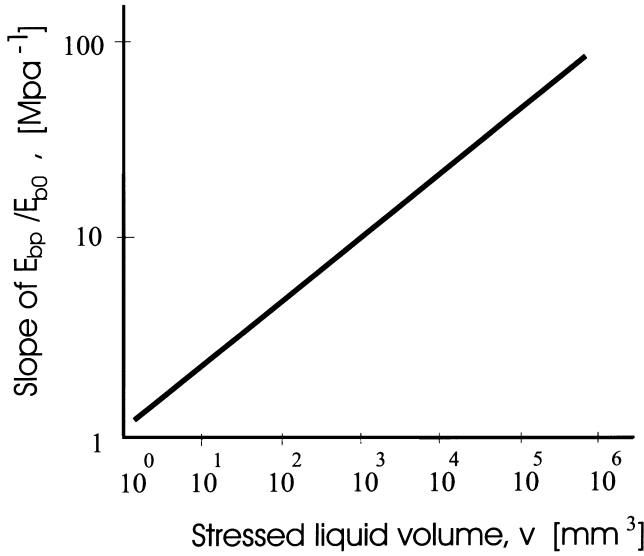


Figure 21 Initial slope of E_{bp}/E_{b0} vs stressed liquid nitrogen volume

stressed volume v , as shown in *Figure 21*. Volume effect degradation may be offset to some extent when relying onto a high pressure in liquid nitrogen.

Non-uniform field breakdown. Highly non-uniform fields are not very favourable to withstand high voltages in cryogenic liquids. Point electrode gap configurations should be suppressed at best in practice. For a point to plane configuration (spacing d in mm; V_b in kV)

$$V_b = 7d^{0.4} \quad (7)$$

has been found to indicate breakdown in normal boiling liquid helium. In case of normal boiling liquid nitrogen the relation

$$V_b = 18d^{0.26} \quad (8)$$

may be used³. These formulas may be relevant up to $d < 10$

mm. Corona can arise before breakdown, especially when stressing the gap with a.c. voltage. Note that negative ion shielding also occurs in liquid helium since the electrons are virtually trapped²³. No formula is known for liquid neon. A concurrent diagram to *Figure 18* has been established for a point to plane gap with 1 mm spacing⁵⁰, see *Figure 22*. The maximum withstand voltage of ≈ 17.5 kV is not related to a maximum density number at all; this may elucidate the complexity of breakdown in non-uniform field gaps.

Solid insulants

Insulating solids have to meet various needs

1. They must hold conductors in position, often under high mechanical stress. Conductor moving can be very harmful to superconductors, e.g. in a magnet.
2. Insulation performance, i.e. resistivity, dielectric strength, aging, must be adequate. Dielectric losses are a key point in a.c. applications. Heat conductivity must be adequate to remove losses to a cooled surface.
3. Solid insulators must be compatible with cryogenics or with high vacuum, respectively.
4. Thermal contraction must be passable.
5. Manufacturing expenditure must be reasonable.

Some of the dielectric phenomena can be merely described by practically intrinsic properties. Resistivity and polarization, respectively, do not suffer from degradation. Discharge onset and breakdown on the other hand depend on extrinsic parameters and can be only extrapolated to a somewhat intrinsic approximation. Solids are usually subjected to a multiples stress, i.e. electrical stress and mechanical stress. The reason for the latter is not only external force stress, but very often simply the thermal contraction mismatch against conductors; an idea about the mismatch can be seen in *Figure 23*.

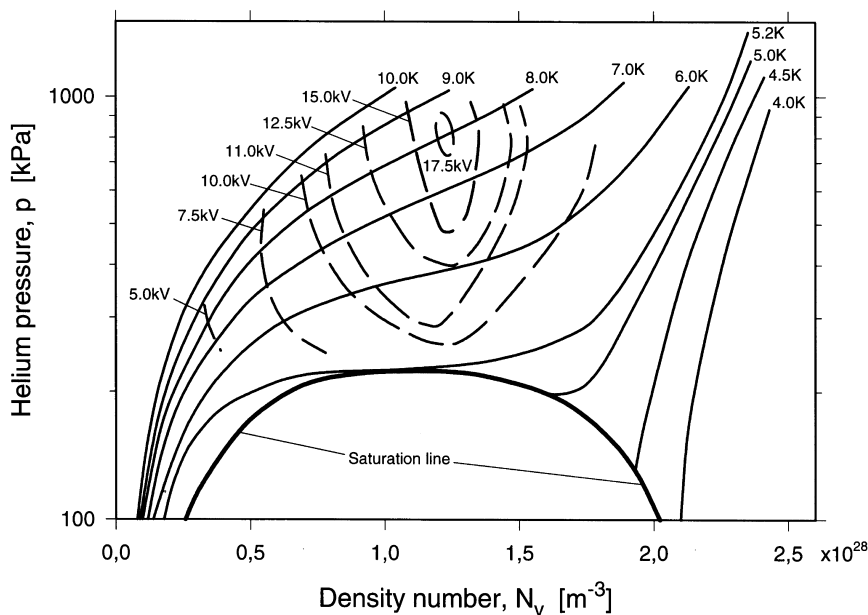


Figure 22 Contour plot of divergent field d.c. breakdown voltages in helium; 1 mm negative point to plane gap

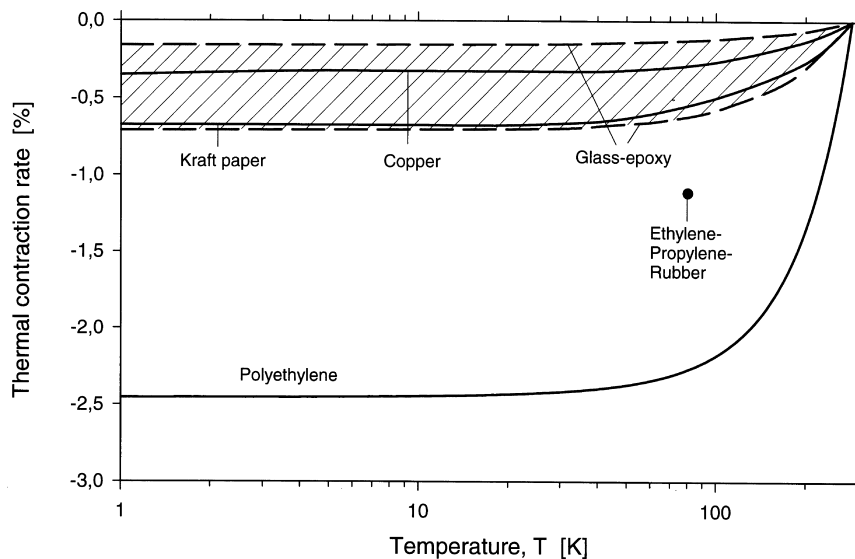


Figure 23 Thermal contraction domains of various solids

Resistivity

Although no net free charges do exist in an ideal insulator, some ions or electrons may move across an imperfect lattice. The corresponding conduction currents often decrease drastically at low temperatures, e.g. with $\exp(-b/T)$ where b is a materials constant and T the temperature⁵¹. The currents decrease with time in general. This indicates a kind of long term polarization.

A high electrical stress may inject additional electrons. An exponential current/voltage relationship often is found at ambient temperature. Space charges can build up in the solid, thereby modifying the internal stress considerably. Very little is known in general about resistivity and space charge build-up at cryogenic temperatures. Figure 24, however, indicates the course of resistivity ρ vs temperature for a polyester varnish⁵². Similar orders have been communicated for glass fibre reinforced epoxies for instance. However, $\rho > 10^{18} \Omega \text{ m}$ has often been claimed for temperatures

$< 50 \text{ K}$. In fact, such a high resistivity is hard to be measured. Nevertheless, this does not mean that charge moving is completely out of question. The situation is analogous to a superconducting wire where a critical current has to be defined by a resistivity criterion for instance, without a distinct limit for genuine superconductivity. Therefore, long term space charge build-up in a cold insulator cannot be excluded completely, and degradation or aging must be encountered with d.c. application. Time constants $\tau_\rho = \epsilon_0 \epsilon_r \rho$ can be extremely long, which can result in quite unusual voltage gradients. These phenomena can result in long term failure of a solid insulator.

Surface conduction, which often gives rise to severe problems at ambient temperature, is of less concern in the cryogenic domain. The causal humidity traces are completely frozen, and ions are immobilized. However, long term d.c. stress may again accumulate surface charges which can affect the original surface voltage gradient considerably. This impairs surface flashover for instance.

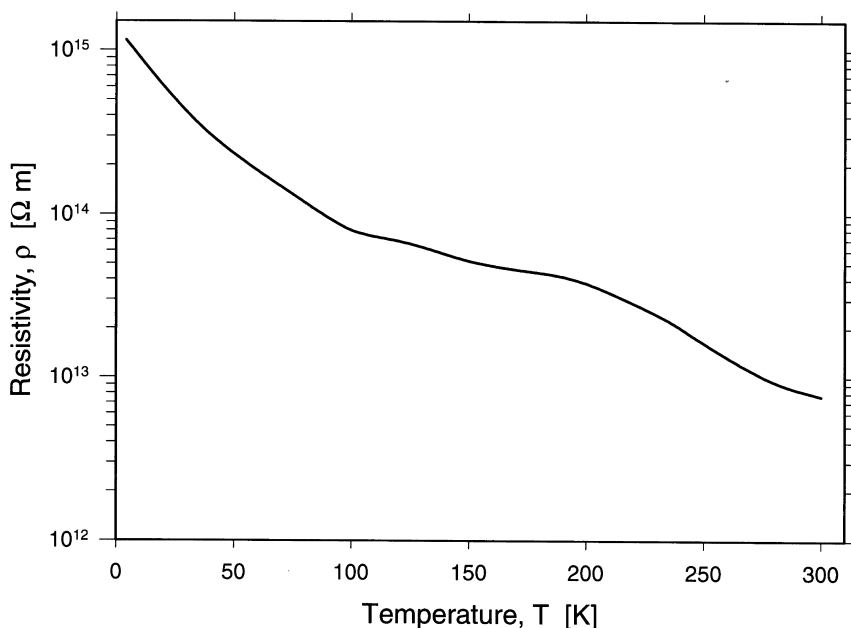


Figure 24 Resistivity of polyester varnish vs temperature

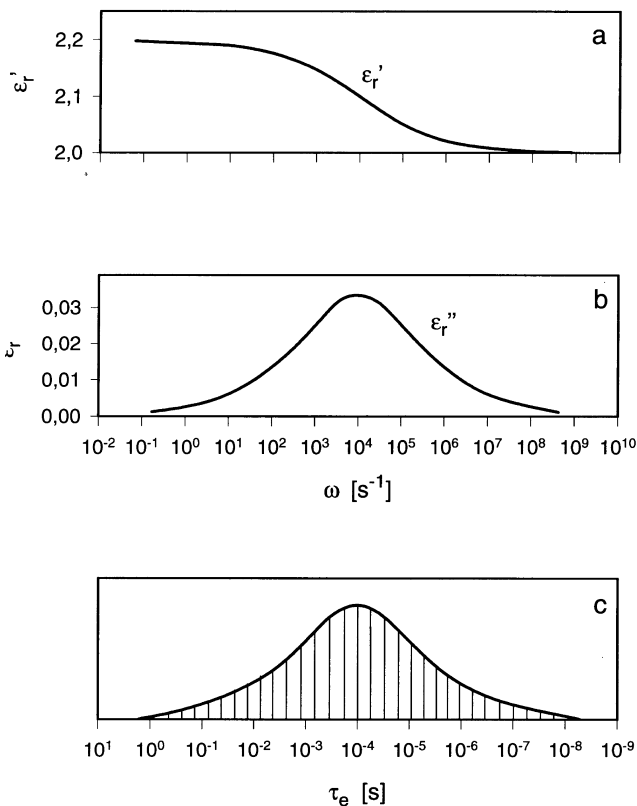


Figure 25 Principal course of complex permittivity (a, b); relaxation time constant is scattered around a central value with a distribution as shown by the shaded area at the bottom (c)

Impurity particles in a cryogen may be the primary source for charge accumulation

Permittivity and dielectric losses

Movement of bound charges in a solid insulator is restricted. Polarization is the net outcome of the charge displacements when an external field is switched on. A relative movement of electrons and nuclei of atoms occurs in all

materials. It is an atomic phenomenon and not influenced by the temperature at all. A relative permittivity of about two is typical for this mechanism. A ionic or partly ionic crystal may show an additional displacement moving of positive and negative ions. Again, temperature often is of little concern. The permittivity range is near five or more. A lot of ceramics belong in this class. Various common plastic materials embody in addition dipolar groups which are turned under electrical stress as a special kind of polarization. Thermal agitation impedes turning, so this polarization increases with the reciprocal of temperature unless a glass-rubber transition freezes the dipoles. Permittivity may be high when polar dipoles are involved. However, there is a strong influence of frequency f^{51} .

Permittivity and dielectric loss characteristics of materials are usually described by means of a complex permittivity $\epsilon_r = \epsilon_r' - j\epsilon_r''$. The dielectric dissipation factor is defined by $\tan\delta = \epsilon_r''/\epsilon_r'$. Dipolar polarization incorporates a relaxation time constant τ_e which may increase considerably at low temperature. The imaginary part ϵ_r'' shows a sharp maximum just around $2\pi f \cdot \tau_e = 1$ in simple materials with only one distinct dipole type. Most solid insulators are composed of various dipolar groups in contrast to this. Hence an extended time constant spectrum must be suspected, and the complex permittivity course is considerably widened around the maximum region⁵¹. This is schematically illustrated in Figure 25.

A correlation between dielectric losses and mechanical damping has been made evident by the way⁵³. This is illustrated for an epoxy in Figure 26. Figure 27 illustrates the typical course of the dielectric loss number vs temperature in a partly polar dielectric which has been used for bushing insulators, for instance⁵⁴; the dielectric losses are proportional to the dielectric loss number $\epsilon_r \cdot \tan\delta$. The characteristics of some other materials can be found in Figures 28 and 29⁵². The mutual interactions in practical solid insulants becomes evident, and the relaxation time constant spectrum may be rather complex. A survey chart for materials of special interest in cryogenics is given in Figures 30 and 31⁵².

The dielectric losses which rise with the square of the

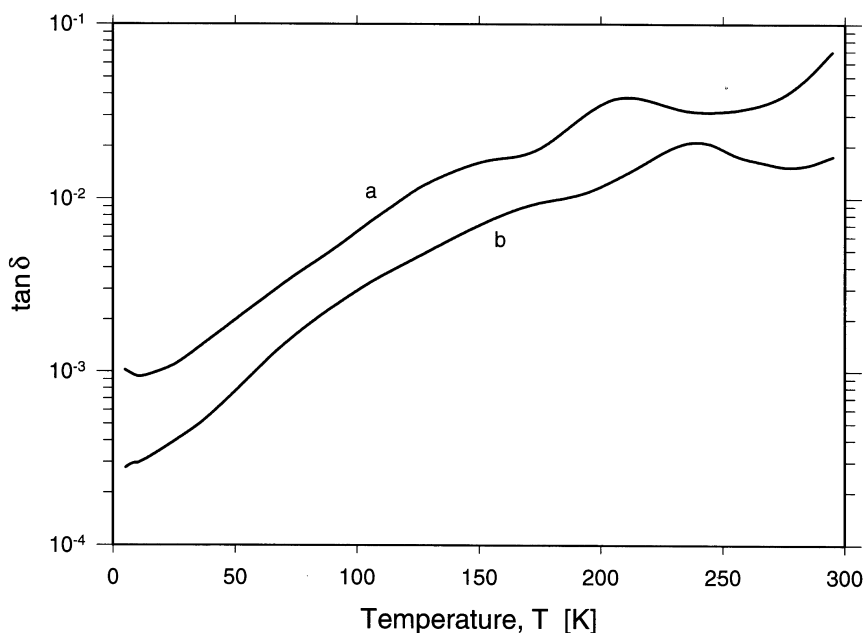


Figure 26 Dielectric loss factor (a), and mechanical loss factor (b), in epoxy (Cy221/Hy979)

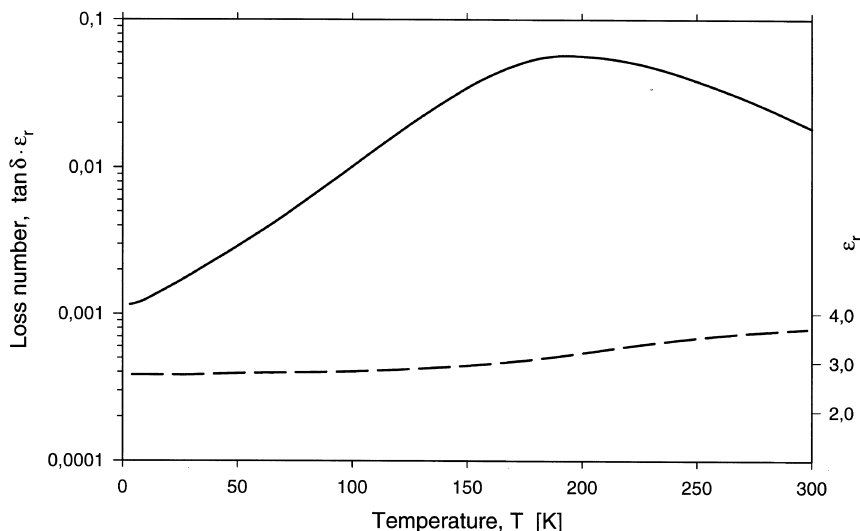


Figure 27 Relative permittivity and dielectric loss number of PERTINAX 100^R at power frequency vs temperature. --- relative permittivity ϵ_r ; — loss number $\epsilon_r \tan \delta$

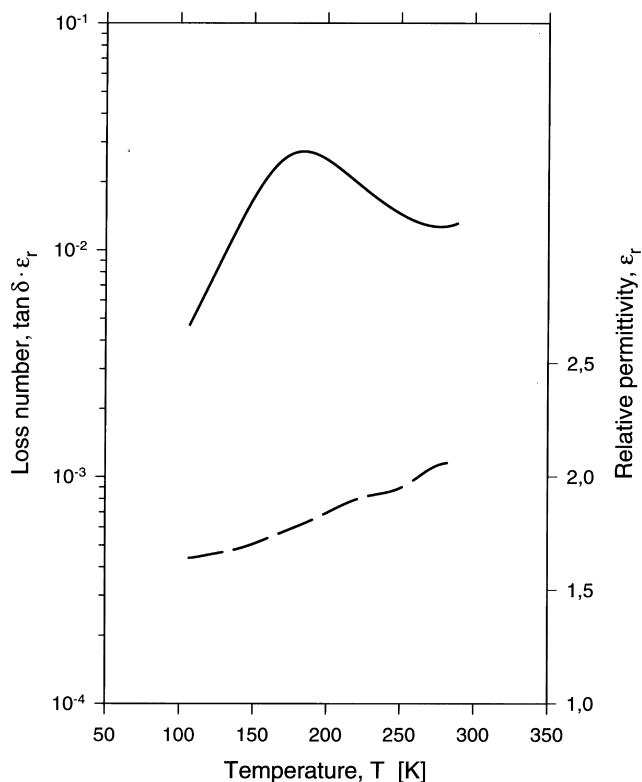


Figure 28 Relative permittivity and dielectric loss number at power frequency vs temperature in dry Kraft paper. --- relative permittivity ϵ_r ; — loss number $\epsilon_r \tan \delta$

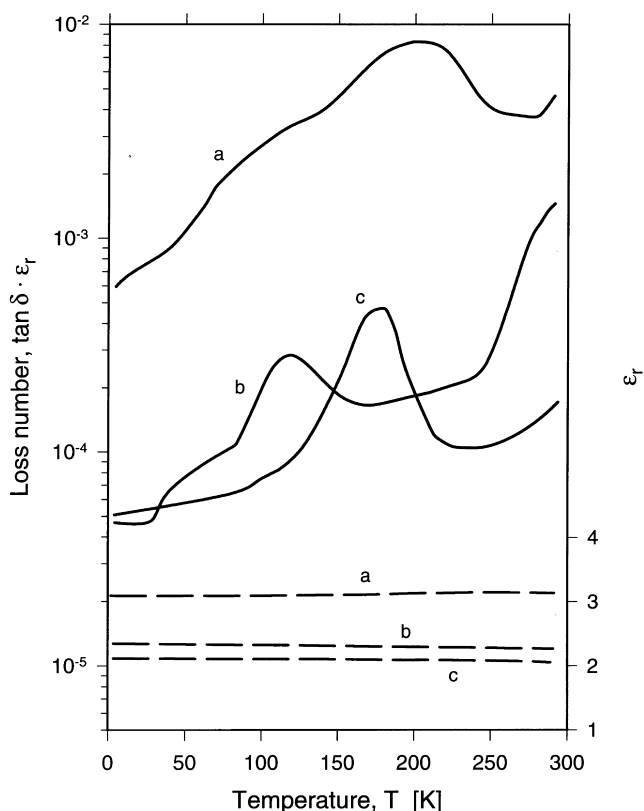


Figure 29 Relative permittivity and dielectric loss number at power frequency vs temperature in various polymers. --- relative permittivity ϵ_r ; — loss number $\epsilon_r \tan \delta$; (a) polyimide; (b) polypropylene; (c) polytetrafluorethylene

stressing voltage have to be removed out of the solid by heat conduction. A thermal instability can even arise at cryogenic temperatures where heat conductivity often is extremely low. The losses may increase when a temperature rise starts, and a final heat breakdown could occur in a thick insulator with a high stressing voltage.

Not only bulk insulators, but also tape materials may be of special interest for a.c. voltage insulation systems. *Table 2* lists materials which have been investigated for use in superconducting a.c. power cables⁵⁵.

Breakdown

A discharge-free arrangement is the first prerequisite when searching for near intrinsic dielectric breakdown, even though a true intrinsic strength has been questioned. Stress level as well as stress duration have a significant influence⁵⁰. As an order of magnitude, some 100 kV mm⁻¹ can be assumed for most insulators for the intrinsic strength. This is considerably higher than in cryogenic liquids. Temperature has limited effect between 300 K and 4 K unless

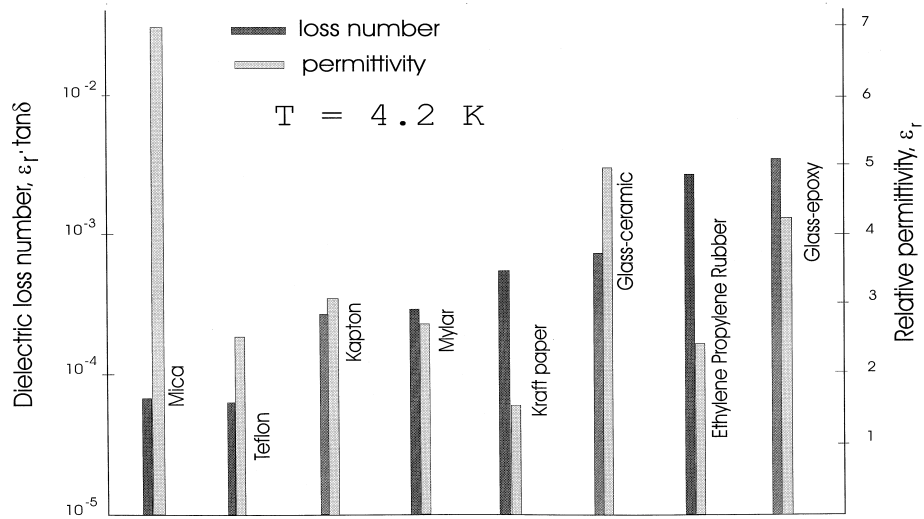


Figure 30 Permittivity and dielectric loss number of various solid insulators at 50 Hz; temperature 4.2 K

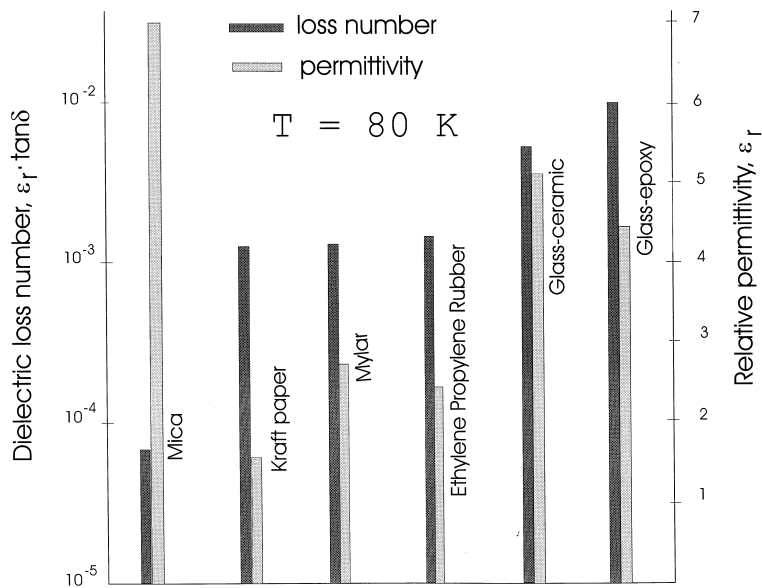


Figure 31 Permittivity and dielectric loss number of various solid insulators at 50 Hz; temperature 80 K

Table 2 Properties of various insulators⁵⁵

Generic material	Temperature 293 K				Temperature 77 K			Temperature 4.2 K			
	ϵ_r	$\tan \delta$ (μrad)	Elastic modulus (Mpa)	Yield strength (Mpa)	$\tan \delta$ (μrad)	Elastic modulus (Mpa)	Yield strength (Mpa)	$\tan \delta$ (μrad)	Elastic modulus (Mpa)	Yield strength (Mpa)	Contraction from 293 K (%)
Low density polyethylene	2.3	200	93	2.1	25	3700	100	15	5500	150	2.7
Oriented polyethylene	2.3	100	890	3.9	30	3900	93	20	4200	125	1.7
Biaxially oriented polypropylene	2.3	200	1900	22	50	1500	180	21	1400	210	0.6
Polysulphone	3.1	800	1900	40		2400	67	60	4500	110	1.2
Polycarbonate	3.0	2100	2150	37		3400	93	55	4100	170	0.5
Polyethylene-terephthalate	3.1	2000	5000	65	800	9300	170	200	10 000	190	1.2
Polyimide	3.1	1700	2900	44	600	4900	110	90	5500	155	0.9

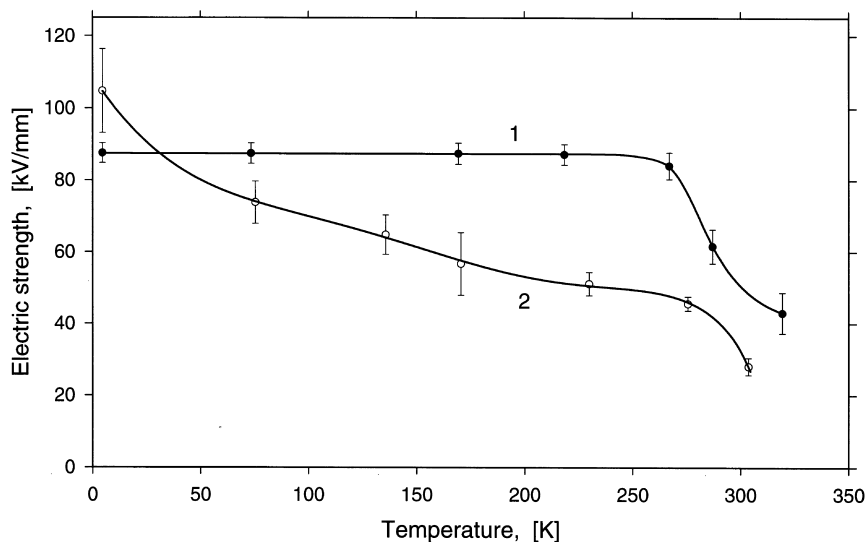


Figure 32 Intrinsic dc breakdown field strength of polymers vs temperature. (1) Low-density polyethylene; (2) ethylene-propylene rubber

a glass–rubber transition occurs. *Figure 32* shows the measured breakdown strength characteristics for two polymer films⁵⁶. Although near intrinsic breakdown is of course a statistical phenomenon, no detailed information is available in the cryogenic domain for the size/long term effect degradation.

Almost one order of magnitude in degradation of bulk solids must be accepted in practice, see for instance *Figure 1*. The withstand strength of some not fully matching solid insulators may in fact be lower than that of liquids. Selected polymers may be classified on the other hand as a kind of cryogenic ‘Super Electrical Insulants’ (SEI) for reasons of the very exciting performance under ideal environmental conditions⁵⁷. Extruded Polyethylene and Ethylene Propylene Rubber are top candidates at present.

External effects can be harmful in any way. Breakdown strength in solids suffers considerably from environmental degradation. There are a lot of imperfections in practice. Interface phenomena, for instance, are especially crucial when local high stress points occur where a cryogenic fluid, or a vacuum insulant, is overstressed and partial discharges occur. Treeing in polymers also occurs at cryogenic temperatures, but tree starting voltages may be considerably higher than at ambient temperature⁵⁷. Internal voids as well as electrode adjacent voids are another source for degradation. Apart from manufacturing defects, cracking during cooldown must be envisaged with bulk solids. Glass fibre reinforced epoxies are a well known example. There is no self healing of damaged solids at cryogenic temperatures, so any discharges must be eliminated in normal operation. Partial discharges cause aging of the solid, which often has been found more distinct than at ambient temperatures; the exponent $1/n$ in the life Equation (6) possibly ranging down to $1/100$ ⁵⁸. Thus, even short term high stress in course of a temporary overvoltage can be dangerous, and can affect the lifetime of a cryogenic insulating system considerably, especially when using polymers. No detectable partial discharges may be allowed in normal operation. Only short pulse overvoltages leading to partial discharges may be tolerable; pulse breakdown withstand voltages in general are much higher than long term withstand voltages.

Conclusions

A broad variety of insulating materials is available in the cryogenic temperature domain. All these insulants show fairly good intrinsic properties, i.e. may perform very well under carefully controlled laboratory test conditions in small scale, short term experiments. However, superconducting power apparatus are rather large and must have a usual life of an order of 30 years. Hence, the insulant performance must be extrapolated to large dimensions and long term stress in order to define conditions for a near zero failure probability. Although knowledge about extrapolation often is still fragmentary, some matching thumb-rules may be established to come to a satisfying withstand voltage estimation without being forced to introduce excessive safety factors.

References

1. Hara, M. and Gerhold, J., Electrical insulation specification and design method for superconducting power equipment. *Cryogenics*, 1998, **38**, this issue.
2. Trump, J. G., Insulation strength of high-pressure gases and of vacuum. In *Dielectric Materials and their Applications*, ed. A. von Hippel. The MIT Press, Cambridge, MA, 1954, pp. 147-156.
3. Gerhold, J., Dielectric properties of cryogenics. In *Handbook of Applied Superconductivity*, Vol. 1/Part D Cooling Technology for Superconductors, ed. B. Seeber. Institute of Physics, Bristol, 1998.
4. Gerhold, J., Electrical insulation in superconducting power systems. *IEEE Electrical Insulation Magazine*, 1992, **8**, 14–20.
5. Krähenbühl, F., Bernstein, B., Danikas, M., Densley, J., Kadotani, K., Kahle, M., Kosaki, M., Mitsui, H., Nagao, M., Smit, J. and Tanaka, T., Properties of electrical insulating materials at cryogenic temperatures: a literature review. *IEEE Electrical Magazine*, 1994, **10**, 10–22.
6. Fengnian, H. and Weihan, W., Electrical breakdown of vacuum insulation at cryogenic temperature. *IEEE Transactions on Electrical Insulation*, 1990, **25**(3), 557–562.
7. Thompson, J. E., Vacuum insulation, conduction, recovery, and application: a review. *6th ISH*, New Orleans/LA, 1989, pp. 48.01/1-01/10.
8. Bobo, J. C., Poitevin, J. and Nithart, H., Tenue diélectrique des isolants à 4,2 K. *CIGRE-Symposium S05-87*, Vienna/Austria, 1987, pp. 100-04/1-04/4.
9. Looms, J.S.T., Meats, R.J. and Swift, D.A., Vacuum insulation

- between very cold niobium electrodes. *Brit. J. Appl. Phys. (J. Phys. D)*, 1968, **1**(2), 377–379.
10. Halbritter, J., Dynamical enhanced electron emission and discharges at contaminated surfaces. *Appl. Phys. A*, 1986, **39**, 49–57.
 11. Schauer, F., Über die Anwendung von Hochvakuum zur thermischen und elektrischen Isolierung elektrischer Hochspannungseinrichtungen bei tiefen Temperaturen. Doctorate thesis, Technical University Graz, Austria, 1979.
 12. Batrakov, A.V., Nazarov, D.S., Ozur, G.E., Popov, S.A., Proskurovsky, D.I. and Rotshtein, V.P., Increasing the electric strength of vacuum insulation by irradiating the electrodes with a low-energy high-current electron beam. *IEEE Transactions on Dielectrics and Electrical Insulation*, 1997, **4**(6), 857–862.
 13. Farall, G.A., Electrical breakdown in vacuum. *IEEE Transactions on Electrical Insulation*, 1985, **20**(5), 815–841.
 14. Mazurek, B. and Cross, J.D., An energy explanation of the area effect in electrical breakdown in vacuum. *IEEE Transactions on Electrical Insulation*, 1987, **22**(3), 341–346.
 15. Schmidt, B. D., Influence of electrode curvature on breakdown voltage of high vacuum gaps. *8th Int. Symp. on Discharges and Electrical Insulation in Vacuum*, Albuquerque, USA, 1978.
 16. Osmokrovic, P. and Djogo, G., Applicability of simple expressions for electrical breakdown probability in vacuum. *IEEE Transactions on Electrical Insulation*, 1989, **24**(6), 943–947.
 17. Hara, M. and Suehiro, J., Improvement of dielectric performance of electrically and magnetically stressed vacuum gaps by controlling electron moving. *6th ISH*, New Orleans, USA, 1989, pp. 48.08/1-48.08/4.
 18. Gerhold, J. and Hara, M., Insulation of high critical temperature superconducting power equipment with liquid nitrogen. *Proc. 10th ISH*, vol. 2, Montreal, Canada, 1997, pp. 125-128.
 19. Nelson, R.L., Dielectric loss of liquid helium. *Cryogenics*, 1974, **14**, 345–346.
 20. Cooke, C.M. and Cookson, A.H., The nature and practice of gases as electrical insulators. *IEEE Transactions on Electrical Insulation*, 1978, **13**(4), 239–247.
 21. Dakin, T. W., Gerhold, J., Krasucki, Z., Luxa, G., Oppermann, G., Vigreux, J., Wind, G. and Winkelnkemper, H., Breakdown of gases in uniform fields. In *CIGRE Working Group 15.03 Paris*, France, 1977.
 22. Gerhold, J., Hubmann, M. and Telser, E., Discharges in cold helium gas near the Paschen-minimum region. *Proc. 11th Int. Conf. on Gas Discharges and their Applications*, Tokyo/Japan, 1995, pp. II/76-79.
 23. Hara, M., Suehiro, J. and Matsumoto, H., Breakdown characteristics of cryogenic gaseous helium in uniform electric field and space charge modified non-uniform field. *Cryogenics*, 1990, **30**, 787–794.
 24. Gerhold, J., Dielectric strength of gaseous and liquid insulants at low temperatures. *CIGRE-Symposium S05-87*, Vienna, Austria, 1987, pp. 100-011-016.
 25. Gerhold, J., Dielectric breakdown of cryogenic gases and liquids. *Cryogenics*, 1979, **19**, 571–584.
 26. Vijn, A.K., Some physico-chemical factors determining the relative electric strength of gases. *Materials Chemistry*, 1982, **7**, 57–70.
 27. Gerhold, J., Hubmann, M. and Telser, E., Near Paschen-minimum discharge phenomena in helium gas. *Proc. 12th Int. Conf. on Gas Discharges and their Applications*, Greifswald, Germany, 1997, pp. 252-255.
 28. Hara, M., Suehiro, J. and Matsumoto, H., Breakdown characteristics of cryogen gaseous nitrogen and estimation of its electrical insulation properties. *IEEE Transactions on Electrical Insulation*, 1989, **24**(4), 609–617.
 29. Gallagher, T. J., *Simple Dielectric Liquids*. Clarendon Press, Oxford, 1975.
 30. Yoshino, K., Ohseko, K., Shiraiishi, M., Terauchi, M. and Inuit, Y., Dielectric breakdown of cryogenic liquids in terms of pressure, polarity, pulse width and impurity. *Journal of Electrostatics*, 1982, **12**, 305–314.
 31. Okubo, H., Goshima, H., Hayakawa, N. and Hikita, M., High voltage insulation of superconducting power apparatus. *Proc. 9th ISH*, Graz/Austria, 1995, pp. 9007/1-9007/12.
 32. Gerhold, J., Liquid helium breakdown as function of temperature and electrode roughness. *IEEE Transactions on Dielectrics and Electrical Insulation*, 1994, **1**(1), 432–439.
 33. Peier, D., Breakdown of LN2 by field induced microbubbles. *Journal of Electrostatics*, 1979, **7**, 113–122.
 34. Gerhold, J., Breakdown phenomena in liquid helium. *IEEE Transactions on Electrical Insulation*, 1989, **24**(2), 155–166.
 35. Weibull, W., A statistical theory of the strength of materials. *Ingenjörsvetenskapsakademiens Handlingar* Nr. 151, Stockholm, Sweden, 1939.
 36. Gerhold, J., Hubmann, M. and Telser, E., Gap size effect on liquid helium breakdown. *Cryogenics*, 1994, **34**, 579–586.
 37. Gerhold, J., Hubmann, M. and Telser, E., Breakdown probability and size effect in liquid helium. *IEEE Transactions on Dielectrics and Electrical Insulation*, 1998, **5**, 321–333.
 38. Suehiro, J., Ohno, K., Takahashi, T., Miyama, M. and Hara, M., Size effect and statistical characteristics of dc and pulsed breakdown of liquid helium. *IEEE Transactions on Dielectrics and Electrical Insulation*, 1996, **3**(4), 507–514.
 39. Delucchi, M., Girdino, P., Liberti, G. and Molinari, G., A statistical analysis of the ac dielectric strength of liquid nitrogen with IEC spherical electrodes under controlled conditions. *Journal of Electrostatics*, 1982, **12**, 315–322.
 40. Kawashima, A., Electrode area effect on the electric breakdown of liquid nitrogen. *Cryogenics*, 1974, **14**, 217–219.
 41. Centurioni, L., Molinari, G. and Viviani, A., Study of the dielectric behaviour of flowing liquid nitrogen. *RGE*, 1975, **84**, 583–586.
 42. Goshima, H., Hayakawa, N., Hikita, M. and Okubo, H., Weibull statistical analysis of area and volume effects on the breakdown strength in liquid nitrogen. *IEEE Transactions on Dielectrics and Electrical Insulation*, 1995, **2**(3), 385–393.
 43. Wu, J.L., Cryogenic dielectric testing performed for the SMES-ETM program. *Adv. Cryog. Eng.*, 1996, **41**, 1843–1850.
 44. Suehiro, J., Ohno, K., Takahashi, T., Miyama, M. and Hara, M., Statistical characteristics of electrical breakdown in saturated superfluid helium. *Conf. Record 12th Int. Conf. on Conduction and Breakdown in Dielectric Liquids*, Rome, Italy, 1996, pp. 320-323.
 45. Hayakawa, N., Sakakibara, H., Goshima, H., Hikita, M. and Okubo, H., Breakdown mechanism of liquid nitrogen viewed from area and volume effects. *IEEE Transactions on Dielectrics and Electrical Insulation*, 1997, **4**(1), 127–134.
 46. Dissado, L.A., Fothergill, J.C., Wolfe, S.V. and Hill, R.M., Weibull statistics in dielectric breakdown; theoretical basis, applications and implications. *IEEE Transactions on Electrical Insulation*, 1984, **19**(3), 227–233.
 47. Meats, R.J., Pressurized-helium breakdown at very low temperatures. *Proc. IEE*, 1972, **119**, 760–766.
 48. Hwang, K. F., Dielectric strength of helium vapour and liquid at temperatures between 1.4 and 4.2 K. *Adv. Cryog. Eng.*, 1977, **8**, 110-117.
 49. Hara, M., Suehiro, J., Tachibana, Y., Takeo, M., Kosaki, M., Hoshino, M., Satow, T., Yamamoto, J., Motojima, O., Breakdown characteristics of pressurized superfluid He II. *Proc. 8th ISH*, vol. 2, Yokohama, Japan, 1993, pp. 559-562.
 50. Hara, M., Electrical insulations in superconducting apparatus. *Cryog. Eng. Japan*, 1989, **24**, 72–81.
 51. Sillars, R. W., *Electrical Insulating Materials and their Applications*. Peter Peregrinus, Stevenage, 1973.
 52. Gerhold, J., Dielectric properties. In *Handbook of Applied Superconductivity*, Vol. 1/part F Materials at low Temperatures, ed. B. Seeber. Institute of Physics, Bristol, 1998.
 53. Hartwig, G. and Schwarz, G., Correlation of dielectric and mechanical damping. *Adv. Cryog. Eng.*, 1984, **30**, 61–70.
 54. Schauer, F., A capacitance-graded cryogenic high voltage bushing for vertical or horizontal mounting. *Cryogenics*, 1984, **24**, 90–96.
 55. Forsyth, E.B., The dielectric insulation of superconducting power cables. *Proc. IEEE*, 1991, **79**, 31–40.
 56. Mizuno, Y., Nagao, M., Kosaki, M., Shimizu, N. and Horii, K., Evaluation of Ethylene-Propylene rubber as electrical insulating materials for a superconducting cable. *IEEE Transactions on Electrical Insulation*, 1992, **27**(6), 1108–1117.
 57. Kosaki, M., Nagao, M., Shimizu, N. and Mizuno, Y., Solid insulation and its deterioration. *Cryogenics* **38**, 1998 (this issue).
 58. Bulinski, A., Densley, J. and Sudarshan, T.S., The ageing of electrical insulation at cryogenic temperatures. *IEEE Transaction on Electrical Insulation*, 1980, **15**(2), 83–88.